METHANE ADSORPTION BY CARBON MOLECULAR SIEVE DERIVED FROM POLYCARBONATE AND POLYANILINE

Jakchai Thawornwatthanasirikul

A Thesis Submitted in Partial Fulfillment of the Requirements
for the Degree of Master of Science
The Petroleum and Petrochemical College, Chulalongkorn University
in Academic Partnership with
The University of Michigan, The University of Oklahoma,
Case Western Reserve University, and Institut Français du Pétrole
2017

บทคัดย่อและแฟ้มข้อมูลฉบับเต็มของวิทยานิพนธ์ตั้งแต่ปีการศึกษา 2554 ที่ให้บริการในคลังปัญญาจุฬาฯ (CUIR)
เป็นแฟ้มข้อมูลของนิสิตเจ้าของวิทยานิพนธ์ที่ส่งผ่านทางบัณฑิตวิทยาลัย
The abstract and full text of theses from the academic year 2011 in Chulalongkorn University Intellectual Repository(CUIR)
are the thesis authors' files submitted through the Graduate School.

Thesis Title:	Methane Adsorption by Carbon Molecular Sieve Derived from Polycarbonate and Polyaniline
By:	Jakchai Thawornwatthanasirikul
Program:	Petroleum Technology
Thesis Advisors:	Assoc. Prof. Boonyarach Kitiyanan Prof. Pramoch Rangsunvigit Dr. Santi Kulprathipanja

---

Accepted by The Petroleum and Petrochemical College, Chulalongkorn University, in partial fulfillment of the requirements for the Degree of Master of Science.

..... College Dean
(Prof.Suwabun Chirachanchai)

Thesis Committee:

.....	.....
(Dr. Ampira Charoensaeng)	(Assoc. Prof. Boonyarach Kitiyanan)
.....	.....
(Prof. Pramoch Rangsunvigit)	(Dr. Santi Kulprathipanja)

.....
(Dr. Sitthiphong Pengpanich)

ABSTRACT

5873006063: Petroleum Technology Program
Jakchai Thawornwatthnasirikul: Methane Adsorption by Carbon Molecular Sieve Derived from Polycarbonate and Polyaniline.
Thesis Advisors: Assoc. Prof. Boonyarach Kitiyanan, Prof. Pramoch Rangsunvigit, and Dr. Santi Kulprathipanja, 59 pp.
Keywords: Methane(CH_4)/ Adsorption/ Carbon molecular sieve (CMS)/ Polycarbonate (PC)/ and Polyaniline (PANI)

The adsorptions of methane by carbon molecular sieves (CMS) were investigated at 35°C and 45°C by volumetric apparatus with the pressure range from 0 to 800 psia. CMS was prepared from polymer precursors such as polycarbonate (PC) and polyaniline (PANI) by carbonization under nitrogen inert atmosphere and activation by CO_2 at temperature 700, 800 and 900°C. The yield of CMS is decreased with increasing carbonization and activation temperature. The methane adsorption capacity at 35°C of CMS derived from PC is 2.82 mmol CH_4/g. The methane adsorption of the samples from PC is higher than those obtained from PANI for the same carbonization and activation. It is interesting to note that the CMS derived from 700 °C carbonization and activation of PC is higher than the samples obtained from 800 and 900°C carbonization and activation. As expected, methane adsorption at 35°C is higher than that at 45°C for all samples. BET surface area and pore analysis was used to characterize the physical properties and relate to the adsorption capacity.

บทคัดย่อ

จักรชัย ถาวรวัฒนสิริกุล: การดูดซับก๊าซมีเทนด้วยคาร์บอนโมเลกุลล่าซีฟ ที่ผลิตจากพอลิคาร์บอเนตและพอลิอะนิลีน (Methane Adsorption by Carbon Molecular Sieve Derived from Polycarbonate and Polyaniline) อ.ที่ปรึกษา: รศ. ดร.บุนยรัชต์ กิติยานันท์ รศ. ดร. ปราโมช รังสรรค์วิจิตร และ ดร.สันติ กุลประทีปัญญา 59 หน้า

การศึกษาหาค่าการดูดซับก๊าซมีเทนด้วยคาร์บอนโมเลกุลล่าซีฟที่อุณหภูมิ 35 และ 45 องศาเซลเซียส ด้วยเครื่องมือการหาค่าแบบ Volumetric ภายใต้ความดันสูงถึง 800 ปอนด์ต่อตารางนิ้ว คาร์บอนโมเลกุลล่าซีฟที่ใช้ในการทดลองนี้ผลิตมาจากสารตั้งต้นที่เป็นพอลิเมอร์ โดยนำพอลิคาร์บอเนตหรือพอลิอะนิลีน มาผ่านกระบวนการคาร์บอไนเซชันโดยใช้ก๊าซไนโตรเจนภายใต้ความดันบรรยากาศที่อุณหภูมิ 700, 800 หรือ 900 องศาเซลเซียส ต่อจากนั้นจึงใช้การกระตุ้นทางกายภาพด้วยก๊าซคาร์บอนไดออกไซด์ที่อุณหภูมิเดียวกันอีก 1 ชั่วโมง จากผลการทดลองพบว่าผลผลิตที่ได้จะลดลงเมื่ออุณหภูมิที่ใช้ในการทดลองนั้นสูงขึ้น ซึ่งเป็นที่น่าสนใจว่าค่าการดูดซับก๊าซมีเทนที่อุณหภูมิ 35 องศาเซลเซียสด้วยคาร์บอนโมเลกุลล่าซีฟที่ได้จากพอลิคาร์บอนเนตด้วยวิธีการคาร์บอไนเซชันและการกระตุ้นที่อุณหภูมิ 700 องศาเซลเซียสนั้นมีค่าสูงที่สุด คือ 2.82 มิลลิโมลก๊าซมีเทนต่อกรัมคาร์บอน จากผลการทดลองเป็นที่น่าสังเกตว่าคาร์บอนโมเลกุลล่าซีฟที่ผลิตจากพอลิคาร์บอเนตจะสามารถดูดซับก๊าซมีเทนได้มากกว่าคาร์บอนโมเลกุลล่าซีฟที่ผลิตจากพอลิอะนิลีนที่ใช้อุณหภูมิเดียวกัน ส่วนปัจจัยเรื่องอุณหภูมิที่ใช้ในการดูดซับก๊าซมีเทนนั้นจากผลการทดลองพบว่าตัวอย่างจะสามารถดูดซับก๊าซมีเทนที่อุณหภูมิ 35 องศาเซลเซียสได้มากกว่าที่อุณหภูมิ 45 องศาเซลเซียส คาร์บอนโมเลกุลล่าซีฟที่เตรียมได้นั้น จะถูกนำไปทดสอบสมบัติทางกายภาพด้วยเครื่องมือวิเคราะห์พื้นที่ผิวบีอีที (BET surface analysis) เพื่อหาความสอดคล้องกับปริมาณการดูดซับก๊าซมีเทน

ACKNOWLEDGEMENTS

First of all, I would like to express my deepest appreciation to my advisor, Assoc. Prof. Boonyarach Kitiyanan, and my co-advisors, Assoc. Prof. Pramoch Rangsunvigit and Dr. Santi Kulprathipanja for their valuable guidance, encouragement, and understanding throughout this research. Their positive attitudes contributed significantly to inspire and maintain my enthusiasm throughout the whole period. I am proud to be their student.

I would like to sincerely thank Dr. Ampira Chareonsaeng and Dr. Sitthiphong Pengpanich for kindly serving on my thesis committee. Their sincere suggestions are definitely imperative for accomplishing my thesis. Additionally, I would like to thank Asst. Prof. Stephan Thierry Dubas for his kindly encouragement and support in this research.

In addition, I would like to thank Ms. Pimchaya Luangaramvej and Mr. Katipot Inkong for their assistance and suggestions.

I am grateful for the partial scholarship and partial funding of the thesis work provided by the Petroleum and Petrochemical College, Center of Excellence on Petrochemical and Materials Technology and Grant for International Integration: Chula Research Scholar, Ratchadaphiseksomphot Endowment Fund, Chulalongkorn University, Thailand.

My gratitude is also extended to all staffs of the Petroleum and Petrochemical College, Chulalongkorn University, for their kind assistance and cooperation.

Furthermore, I would like to thank all of my friends for their friendly assistance, creative suggestions, and encouragement. I had a very good time working with them all.

Finally, I would really like to express my sincere gratitude to my family, especially my parents, for their love, understanding and infinite support.

TABLE OF CONTENTS

		PAGE
Title Page		i
Abstract (in English)		iii
Abstract (in Thai)		iv
Acknowledgements		v
Table of Contents		vi
List of Tables		viii
List of Figures		ix
CHAPTER		
I	**INTRODUCTION**	1
II	**LITERATURE REVIEW**	3
	2.1 Natural Gas	3
	2.2 Natural Gas Storage	4
	2.2.1 Compressed Natural Gas (CNG)	4
	2.2.2 Liquefied Natural Gas (LNG)	4
	2.2.3 Adsorbed Natural Gas (ANG)	5
	2.3 Gas Adsorption	5
	2.3.1 Isotherm Gas Adsorption	6
	2.3.2 Constant Volume Method	8
	2.4 Type of Adsorbent	8
	2.4.1 Activated Carbon (AC)	9
	2.4.2 Carbon Molecular Sieve (CMS)	10
	2.5 Literature Reviews	12
	2.5.1 Carbonization and Activation	13
	2.5.2 Methane Adsorption	17
III	**EXPERIMENTAL**	20

CHAPTER **PAGE**

3.1 Materials and Equipment 20
3.1.1 Materials and Chemicals 20
3.1.2 Equipment 20
3.2 Experimental Procedures 21
3.2.1 Preparation of Polymer Precursor 21
3.2.2 Preparation of Carbon Molecular Sieve 21
3.2.3 Characterization 22
3.2.4 Methane Adsorption 24
3.3 Adsorption and Calculation 26
3.3.1 Static Adsorption 26

IV RESULTS AND DISCUSSIONS 29
4.1 Production of CMS 29
4.1.1 Effect of Polymer Precursor 29
4.1.2 Effect of Carbonization and Activation Temperature 29
4.2 BET Surface Area and Pore Analysis 30
4.3 Methane Adsorption 34

V CONCLUSIONS AND RECOMMENDATIONS 43
5.1 Conclusions 43
5.2 Recommendations 44

REFERENCES 45

APPENDIX 52
The Methane Adsorption Capacity on Each Adsorbent at Temperature of 35ºC and 45ºC 52

CURRICULUM VITAE 59

LIST OF TABLES

TABLE		PAGE
2.1	Pyrolysis temperature ranges and precursor materials for CMS membranes	13
4.1	Yield of products after carbonization and activation at 700, 800 and 900°C	30
4.2	The BET surface area and pore analysis of CMS obtained from polycarbonate and polyaniline by carbonization and activation at temperature 700, 800 and 900°C	31
4.3	The structural properties of adsorbents before and after CVD of methane	34
4.4	The methane adsorption capacity (mmol/g) at 800 psi at 35 and 45°C	37
4.5	The methane adsorption capacity per BET surface area (mmol/m^2) and the methane adsorption capacity per micropore volume (mmol/m^3) at 800 psi and different activation temperature	42

LIST OF FIGURES

FIGURE		PAGE
2.1	Types of physisorption isotherms on IUPAC standard.	8
2.2	Pore size classification on IUPAC standard.	10
2.3	Comparison of (a) a well-ordered structure of graphite and (b) hypothetical structure of a carbon molecular sieve.	11
2.4	Monomers for polyimide used as the precursor for carbon molecular sieve membranes: (a) 2,4,6-trimethyl-1,3-phenylenediamine, (b) 3,4:3',4'-biphenyltetracarboxylic acid dianhydride, and (c) 5,5'-[2,2,2,-trifluoro-1-(trifluoromethyl)ethylidene]-bis-1,3-isobenzofurandione.	14
3.1	Schematic of the volumetric apparatus.	25
4.1	Pore size distribution of CMS obtained from polycarbonate by carbonization and activation at 700, 800 and 900°C.	33
4.2	Pore size distribution of CMS obtained from polyaniline by carbonization and activation at 700, 800 and 900°C.	33
4.3	BJH pore size distribution of the produced ACs and CMS from broom corn stalk.	34
4.4	Methane adsorption at 35°C on CMS obtained from polycarbonate and polyaniline by carbonization and activation at temperature 700, 800 and 900°C.	35
4.5	Methane adsorption at 45°C on CMS obtained from polycarbonate and polyaniline by carbonization and activation at temperature 700, 800 and 900°C.	36
4.6	Methane molecules adsorbed on pores.	36
4.7	Methane adsorption (mmol/g) at 800 psi and 35°C as a function of BET surface area (m^2/g).	38
4.8	Methane adsorption (mmol/g) at 800 psi and 35°C as a function miccropore volume (cm^3/g).	38

FIGURE **PAGE**

4.9 Methane adsorption per BET surface area (mmol/m^2) at 800 psi and 35°C with surface area (m^2/g). 39

4.10 Methane adsorption (mmol/g) at 800 psi and 45°C as a function of BET surface area (m^2/g). 40

4.11 Methane adsorption (mmol/g) at 800 psi and 45°C as a function miccropore volume (cm^3/g). 40

4.12 Methane adsorption per BET surface area (mmol/m^2) at 800 psi and 45°C with surface area (m^2/g). 41

CHAPTER I
INTRODUCTION

Natural gas (NG) is an alternative fuel for vehicles and, per unit of energy, it is much cheaper than conventional gasoline and diesel fuel. Furthermore, natural gas is a comparatively clean burning fuel. However, methane is the major component in natural gas and, at standard temperature and pressure (STP) condition, it is in gas phase and its volumetric energy density is only 0.11% of gasoline. Several methods have been considered in order to increase the energy density for facilitating its use as a vehicular fuel. Compressed natural gas (CNG) has been widely used to store natural gas onboard for car, truck and bus. Nevertheless, the use of CNG has some disadvantages. The CNG storage tanks need to be very strong and therefore very heavy to withstand the high pressure requirement. Moreover, even at high pressure (200 bars), CNG has a lower energy density relative to other liquid vehicle fuels. Therefore, CNG vehicle needs to be refueled more often. In order to overcome its drawback, the high surface area adsorbent such as microporous material is suggested to use to enhance capacity of natural gas storage.

Carbon adsorbent with high adsorption capacity can be produced from a variety of sources, such as gas phase reactions (e.g. carbide derived carbons via chemical vapor deposition), pyrolysis of biomasses (e.g. coal, wood, carbonaceous agricultural waste) and pyrolysis of synthetic precursors (e.g. polyvinylidene chloride, polyimide, phenolic resin). One of the most interesting ways to prepare material is pyrolysis of synthetic precursors because it can be obtained CMS that consisted of smaller pore size with a narrower pore size distribution than other method. However, it is still required to investigate the synthetic precursor and other significant factors corresponding to methane adsorption capacity.

The purpose of this study is to prepare CMS derived from polymer precursor that enhances the methane adsorption ability. Polycarbonate (PC) and polyaniline (PANI) were chosen to use as polymer precursor to prepare CMS. Each sample was carbonized under nitrogen inert atmosphere at desired temperature; 700, 800 or 900°C for 1 h before further activated by CO_2 at the same temperature and

1 h holding time. After activation, the sample was left to cool to the ambient temperature under nitrogen inert atmosphere. Finally, the sample was ground and sieved to the mesh size between 20 and 40 before dried in the oven and kept in the desiccators for methane adsorption test and characterization. The adsorptions of methane on CMS were investigated at 35°C and 45°C by volumetric apparatus with the pressure up to 800 psi. BET surface area was used to characterize the physical properties and related to the adsorption capacity.

CHAPTER II
LITERATURE REVIEW

2.1 Natural Gas

Natural gas (NG) occurs deep beneath the earth's surface. Natural gas is a fossil fuel used as a source of energy for heating, cooking, and electricity generation. It is also used as fuel for vehicles and as a chemical feedstock in the manufacture of plastics and other commercially important organic chemicals. The fact that natural gas is combustible and burns more cleanly than some other energy sources helps reinforce its position as one of the most highly used energy sources.

Natural gas is a naturally occurring hydrocarbongas mixture consisting primarily of methane (CH_4), but commonly including varying amounts of other higher alkanes, and sometimes a small percentage of carbon dioxide, nitrogen, hydrogen sulfide, or helium.

Methane is the main component of NG and represents about two-thirds of the fossil fuels on earth, although it remains the least utilized fuel. In present, there is a great interest in expanding about the use of methane for fueling automobiles because of its wide availability and its lower carbon dioxide emission as compared to petroleum (Gándara *et al*., 2014).

However, NG has lower energy density than conventional and other alternative fuels at ambient conditions, which causes the driving range of NG based fuels vehicle to be less than conventional vehicle (Menon and Komarneni, 1998).

The combustion of methane is representing in the equation 2.1. One molecule of methane is reacted with two molecules of oxygen which both are in gaseous form to get one molecule of carbon dioxide in gaseous form and get two molecules of water in liquid form. It is exothermic reaction so the water released is usually be in steam form and energy is released from the reaction -890 kJ/mol (Lee *et al*., 1994).

$$CH_4(g) + 2O_2(g) \rightarrow CO_2(g) + 2H_2O(l) + 890\ kJ/mol \qquad (2.1)$$

2.2 Natural Gas Storage

The transportation and storage of natural gas or methane has been one of the barriers to natural gas utilization. Transportation of gas by pipeline requires large upfront capital, long pay-back periods and inflexibility once constructed. Another option for natural gas transport/storage is in the form of compressed natural gas (CNG), liquefied natural gas (LNG) and adsorbed natural gas (ANG).

2.1.1 Compressed Natural Gas (CNG)

CNG (Compressed Natural Gas) is a gaseous fuel consisting of a mixture of hydrocarbons, mainly methane. Natural Gas is compressed to a pressure of 200 to 250 bars, to form CNG. Colorless, odorless, non-carcinogenic and non-toxic, CNG has a limited flammability range and is lighter than air. It is not a liquid fuel, and is not the same as LPG (Liquefied Petroleum Gas), which consists of propane and butane in liquid form. Superior to petrol, it operates at nearly no cost of conventional fuel in Iran and hence CNG is increasingly becoming popular with automobile owners. Commonly referred to as the green fuel because of its lead free characteristic, it reduces harmful emissions and is non-corrosive, thereby enhancing longevity of the life of spark plugs. Another practical advantage observed in countries where CNG is already in vogue is the extension of life of lubricating oils as the fuel does not contaminate and dilute the crank-case oil (Eftekhari and Farzaneh-Gord, 2009). However, compressed natural gas vehicles require greater amount of space comparing to conventional gasoline powered vehicles (Abhishankar, 2011).

2.1.2 Liquefied Natural Gas (LNG)

LNG is natural gas that has been cooled to the temperature approximately -161ºC at atmospheric pressure that it condenses to a liquid. LNG has the volumetric energy density is approximately 72% of the total gasoline (Solar *et al*., 2010). The density of LNG is around 0.4-0.5 kg/L which depending on temperature, pressure and composition. LNG is shipped in specially designed vessels for long-distance transport to a market which is more economical and for local distribution by truck onshore. Liquefaction also provides the opportunity to store

natural gas for use during high demand periods in areas where geologic conditions are not suitable for developing underground storage facilities.

2.1.3 Adsorbed Natural Gas (ANG)

ANG is alternatively to the CNG for energy storage. A new technology have been developed which gives revolution for the storage of natural gas known as ANG technology. ANG is a technology in which natural gas is adsorbed by a porous adsorbent such as activated carbon at relatively low pressure (7-40 bar) and room temperature. There are many advantage of ANG as following:

(i) Gas storage using ANG allows for reductions in storage pressures allowing more flexible and possibly lighter storage systems to be installed.

(ii) Flatter, shaped tanks can use space much more efficiently than CNG cylinders.

(iii) The volumetric efficiency of ANG storage over more traditional CNG storage cylinders is typically more than 25%.

(iv) ANG storage units can store much more natural gas than an equivalent storage cylinder with CNG at the same pressure.

(v) Lower fuelling pressure coupled with gas storage on a carbon rather than in free space confers real safety benefits in most instances.

(vi) Reduced pressure relative to CNG allows for reductions of up to 50% in infrastructure and operating costs for filling stations.

However, ANG has a poor specific mass that the ratio of useful gas stored is relatively low to total parasitic mass of activated carbon and the container (Abhishankar, 2011).

2.3 Gas Adsorption

Adsorption is process where molecules from the gas phase or from solid solution bind in a condensed layer on a liquid phase. The molecules that bind to surface are called adsorbate while the substance that holds the adsorbate is called adsorbent. The process when the molecule bind is called adsorption. Removal of the molecules from the surface is called desorption (Masel, 1996).

Adsorption at the solid-gas interface can be divided into two broad classes: chemisorption and physical adsorption. Physical adsorption is reversible adsorption by weak interaction only; no covalent bonds between the adsorbent and the adsorbate and heats of physical adsorption are less than 15-20 kilocalories/mole. Chemisorption is adsorption involving stronger interaction between adsorbate and adsorbent usually accompanied by rearrangement of atoms within or between adsorbates, so reaction occurs between the surface of the adsorbent. Heats of chemisorptions are usually in excess of 20-30 kilocalories/mole.

2.3.1 Isothermal Gas Adsorption

An adsorption isotherm is the relationship at constant temperature between the partial pressure of the adsorbate and the amount adsorbed at equilibrium. This varies from zero at $P/P_0=0$ to infinity as P/P_0 reaches 1.

The most common adsorption experiment is the measurement of the relation between the amount of gas adsorbed and the pressure of the gas. For a given gas-solid pair, the amount of adsorbed gas at equilibrium is a function of pressure and temperature as the following,

$$V=f(P,T) \qquad (2.2)$$

Where V may be expressed in cc STP/g. At a fixed temperature, V is only a function of P, which is called an adsorption isotherm (Yang, 1987).

Isotherm can be classified into six types by IUPAC standard adsorption isotherms as illustrated in Figure 2.1. Adsorption isotherm is a relationship between the amount of adsorption and relative pressure at constant temperature. The horizontal axis is the relative pressure and vertical axis is the amount of adsorption which measure as mmol/g on the standard gas volume (at 0 °C and 1 atm).

Type I isotherm or Langmuir isotherm where the amount of gas increases with increasing pressure and then saturates at about a monolayer coverage It is given by microporous solids structure that relative on the small external surfaces

such as activated carbons, molecular sieve, zeolites and certain porous oxides. The limiting uptake is controlled by the amount of micropore volume more than the internal surface area. It is characteristic of monolayer adsorption.

Type II isotherm is an isotherm where point B in Figure 2.3 is the beginning of linear middle section of the isotherm which indicate the stage of monolayer coverage complete and multilayer adsorption began. Type II isotherm is characteristic of multilayer adsorption.

Type III is an adsorption isotherm which starts from a very little amount of adsorption. However, once a small droplet or island of adsorbate nucleates on the surface, additional adsorption occurs more easily because of strong adsorbate-adsorbent interactions that play an important role as driving force for the adsorption process.

Type IV isotherm appear a hysteresis loop, which is commonly associated with the capillary condensation that take place in mesopores, and the limiting uptake over a range of high relative pressure. The initial part of the Type IV isotherm is attributed to monolayer-multilayer adsorption because it follows the same path as the corresponding part of a Type II isotherm which obtained the given adsorptive on the same surface area of the adsorbent in a non-porous form. In addition, Type IV isotherms use in mesoporous industrial adsorbents.

Type V isotherm is characteristic of the weak adsorbate-adsorbent interaction. This isotherm is indicated about microporous or mesoporous solids. Initially, the adsorption looks like type III adsorption, but eventually the adsorbed layers get so thick as they fill up the pores. As a result, no more gas can be adsorbed and the isotherm is saturated (Masel, 1996).

Type VI isotherm or hypothetical isotherm, in which the sharpness of the steps depends on the system and the temperature, presents the stepwise multilayer adsorption on a uniform non-porous surface. The step-height shows the monolayer capacity for each adsorbed layer that remains nearly constant for two or three adsorbed layers. One of the best examples of Type VI isotherms are those obtained with argon or krypton on graphitized carbon blacks at liquid nitrogen temperature (Sing *et al.,* 1985).

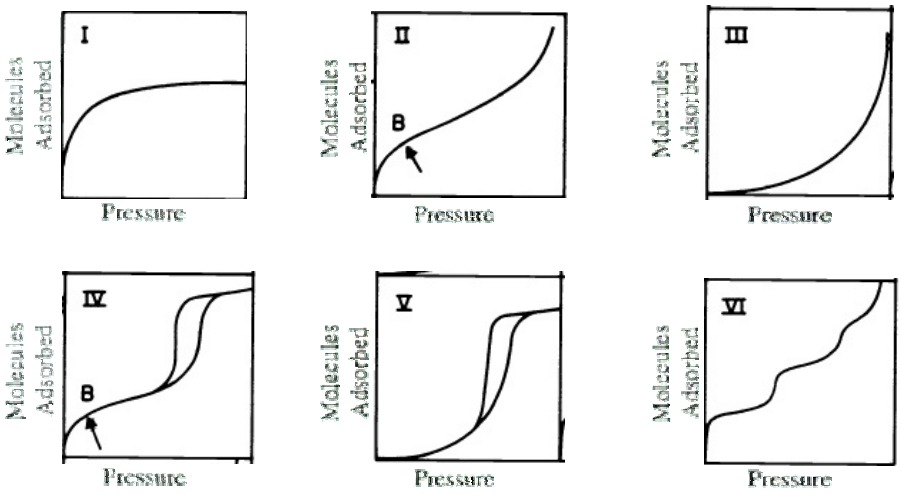

Figure 2.1 Types of physisorption isotherms on IUPAC standard (Sing *et al.,* 1985).

The measurement of pure-gas isotherms is rather straightforward. The amount adsorbed at equilibrium can be determined by two commonly used methods. One is the constant volumetric method, where the pressure before and after adsorption in a closed system is measured. Another is the gravimetric method, in which the amount adsorbed is directly determined by the weight gain in a flow system (Yang, 1987).

2.3.2 Constant-Volume Method

The amount of gas is measured before and after the adsorption takes place. The amount of adsorbed phase is, then calculated by the difference. The pressure and volume, using an appropriate P-V-T relationship can be used to determine the total gas amount. The experimental apparatus contains two compartments can be predetermined by helium displacement. The gas in the reservoir is admitted to the sample compartment, and equilibrium is indicated by the constancy of the pressure (Yang, 1987).

2.4 Type of Adsorbent

The most common commercial adsorbents that provide their uses in gas storage and separation include activated carbon, zeolite and molecular sieves. Some

of the properties that make an adsorbent commercially attractive include high porosity, surface area and total pore volume. The exploited absorbent with respect to these properties is activated carbon. Carbon, by itself, can be regarded in its graphitic form, which its density is equal to 2.25 g/cc although in its disordered crystal state it probably is closer to 2.1 g/cc (Panel, 2000). In order to explore new adsorbents, the focus has now turned to carbon molecular sieve due to their high theoretical surface area and pore size that similar to the molecular dimensions of the adsorbing species. They can become potential adsorbents and competitors to activated carbon.

2.4.1 Activated Carbon

Activated carbons are carbonaceous materials that can be distinguished from elemental carbon by oxidation of the carbon atoms found on the outer and inner surfaces (Mattson and Mark, 1971). These materials are characterized by their extraordinary large specific surface areas, well-developed porosity and tunable surface-containing functional groups (Baker *et al*., 1992, Zong *et al.*, 2003). For these reasons, activated carbons are widely used as adsorbents for the removal of organic chemicals and metal ions of environmental or economic concern from air, gases, potable water and wastewater (El-Hendawy, 2003).

All materials containing high fixed carbon content can potentially be activated. The most commonly used raw materials are coal (anthracite, bituminous and lignite), coconut shells, wood (both soft and hard) peat and petroleum based residues. Most carbonaceous materials do have a certain degree of porosity and an internal surface area in the range of 10-15 m^2/g. During activation, the internal surface becomes more highly developed and extended by controlled oxidation of carbon atoms-usually achieved by the use of steam at high temperature.

After activation, the carbon will have acquired an internal surface area between 700 and 1,200 m^2/g depending on the plant operating conditions. The internal surface area must be accessible to the passage of a fluid or vapor if a potential for adsorption is to exist. Thus, it is necessary that an activated carbon has not only a highly developed internal surface but accessibility to that surface via a network of pores of differing diameters. Pore diameters are usually categorized by IUPAC classification as illustrated in the following:

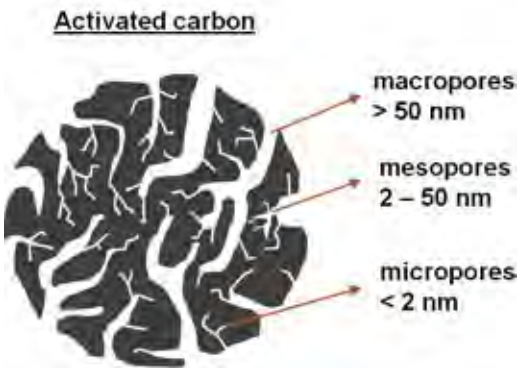

Figure 2.2 Pore size classification on IUPAC standard.

During the manufacturing process, macropores are first formed by the oxidation of weak points (edge groups) on the external surface area of the raw material. Mesopores are then formed and are, essentially, secondary channels formed in the walls of the macropore structure. Finally, the micropores are formed by attack of the planes within the structure of the raw material.

2.4.2 Carbon Molecular Sieve

Molecular sieves can be defined as substances with discrete pore structures that can discriminate between molecules on the basis of size. Carbon molecular sieves (CMS) are a special class of activated carbons. However, pore size distribution of these materials is not always strictly discrete and furthermore, molecules are not hard spheres; they can sometimes squeeze into narrow pores. The distinction between activated or porous carbons and carbon molecular sieves is not clearly defined. Carbon molecular sieves have most of the pores in the molecular size range but some conventional activated carbons also have very small pores. The main distinction is that activated carbons separate molecules through differences in their adsorption equilibrium constants. In contrast, an essential feature of the carbon molecular sieves is that they provide molecular separations based on rate of adsorption rather than on the differences in adsorption capacity. This behavior is clearly evident in pressure swing adsorbers (PSA) where gas dynamics dominate. The separation of nitrogen from air by PSA is the single most important application of CMS.

Carbon molecular sieves are non-crystalline or amorphous and quite unlike inorganic oxide molecular sieves which have a well ordered crystalline structure. A hypothetical structure of a carbon molecular sieve crystallite is shown in Figure 2.3b. Disordered graphitic platelets of carbon are separated by interstitial spaces. The size of the gaps are determined by several factors, such as the presence of foreign atoms between the layers, hanging side groups, and cross-linking chains of carbon atoms. Also influencing the pore structure is the presence of capping groups on the edges of the layers. Also shown in Figure 1a is a well-ordered structure of graphite for comparison purposes.

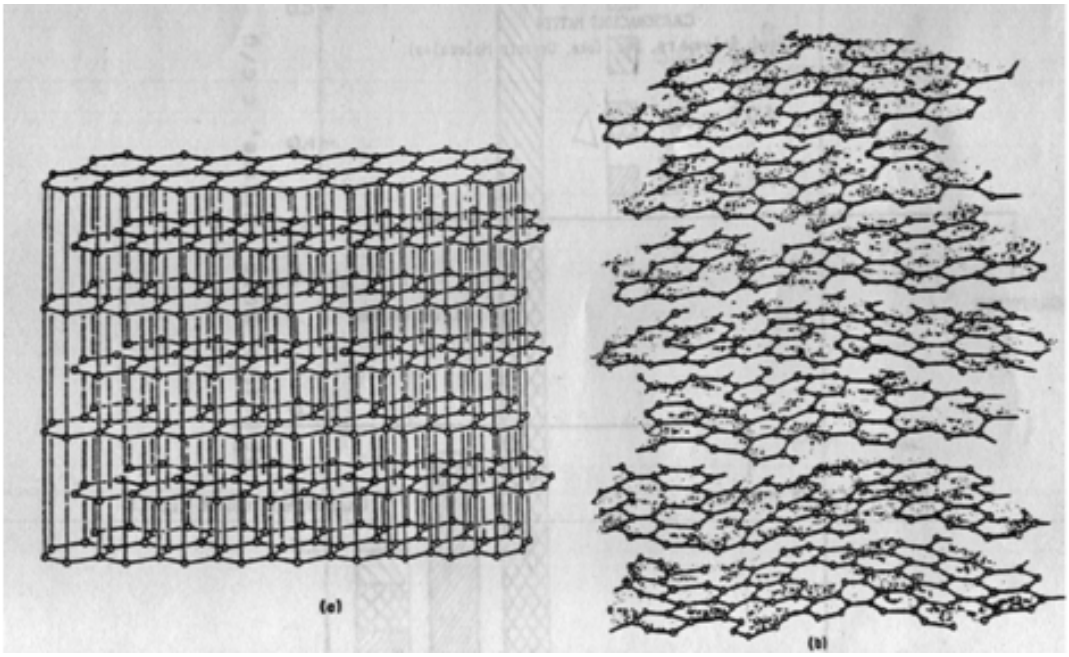

Figure 2.3 Comparison of (a) a well-ordered structure of graphite and (b) hypothetical structure of a carbon molecular sieve (Foley, 1995).

Despite the amorphous nature of carbon molecular sieves, they do show remarkable sieving properties and as such, they have certain advantages over inorganic oxide molecular sieves. These are the following:

(i) Stability at high temperature. It has been reported that some carbon molecular sieves can withstand temperatures up to 1500°C (Walker *et al*., 1966).

(ii) They are stable in acid media. This is an important property in liquid phase operations. The process for purifying terephthalic acid depends on a carbon catalyst with acid stability.

(iii) Carbon sieves have low affinity to water. The property of hydrophobicity can be controlled by the pretreatment conditions during preparation of the sieve; however, most carbon molecular sieves are hydrophobic in character. (Garten and Weiss, 1957).

(iv) Carbon sieves are easy to make, relative to zeolites.

(v) The pore sizes can be controlled by the method of preparation. Oxidation or activation can enlarge them, or they can be decreased by high temperature treatment in an inert atmosphere (Dubinin *et al*., 1961).

2.5 Literature Reviews

Carbon membranes for various separations are typically produced by the pyrolysis of a polymeric precursor. Another synthetic method that has seldom been used is the compression sintering of granular carbon (Ash *et al*., 1976). Both inert purge and vacuum pyrolysis techniques have been used in separate studies but never compared. Soffer *et al*., (1987) produced CMS membranes by use of an argon atmosphere. Hatori *et al*., (1995) produced macroporous carbons by pyrolysis of a Kapton type polyimide film between graphite plates in flowing argon. Chen and Yang, (1994) produced CMS membranes by using a nitrogen atmosphere. Rao and Sircar, (1993) also produced nanoporous membranes by using nitrogen atmosphere. To synthesize carbon hollow fibers, Linkov *et al*., (1994) stabilized and carbonized a polyacrylonitrile/poly-(methyl methacrylate) copolymer in nitrogen. Vacuum pyrolysis was used for CMS hollow fiber membranes (Jones and Koros, 1994 and Haraya and Suda, 1995). To tailor the separation performance of carbon membranes, the pyrolysis temperature can be varied in accordance with the type of precursor material. It is desirable to keep the processing temperature low enough to prevent graphitization, especially for coke-forming precursor materials. For carbon membranes, processing temperatures are typically in the range 500-1000°C, and CMS membrane synthesis temperatures fall within this range (see Table 2.1).

Table 2.1 Pyrolysis temperature ranges and precursor materials for CMS membranes

Researcher	Precursor material	Pyrolysis Temperature(ºC)	Reference
Bird and Trim	Polyfurfuryl alcohol	700	1983
Chen and Yang	Polyfurfuryl alcohol	500	1994
Suda and Haraya	Kapton-type polyimide	500-1000	1995 (2 articles)
Jones and Koros	6F-containing polyimide copolymer	500-550	1994
Soffer *et al.*	Cellulose and derivatives, thermosetting polymers, and peach tar mesophase	800-950	1987

2.5.1 Carbonization and Activation

Geiszler and Koros, (1996) studied the pyrolysis condition of polyimide using either a vacuum pyrolysis or an inert purge pyrolysis technique on a precursor. This polyimide was the product of three monomers: 2,4,6-trimethyl-1,3-phenylenediamine, 3,4:3',4'-biphenyltetracarboxylic acid dianhydride, and 5,5'-[2,2,2,-trifluoro-1-(trifluoromethyl)ethylidene]-bis-1,3-isobenzofurandione whose structures are shown in Figure 2.4 (Jones and Koros, 1994). Additional pyrolysis variables included the type of inert purge gas (argon, helium, and carbon dioxide), purge flow rate, and temperature. Vacuum pyrolysis produced more selective but less productive CMS membranes than the inert purge pyrolyzed membranes. Helium, argon, and carbon dioxide performed as effectively similar purge gases at 550°C, but at 800°C, a carbon dioxide purge produced a highly porous, nonselective membrane by oxidizing the carbon. Reductions in the purge gas flow rate from 200 to 20 cm^3(STP)/min caused a decrease in the permeate flux of the CMS membranes, presumably by the deposition of carbon either on the membrane surface or in the pores. An increase in the pyrolysis temperature from 550 to 800°C caused a

significant decrease in the permeate flux and a significant increase in the selectivity for CMS membranes produced by both vacuum and inert purge pyrolysis techniques. The removal of residual oxygen at the ppm level reduced the apparent pore size of CMS membranes, resulting in higher selectivities and lower permeate fluxes.

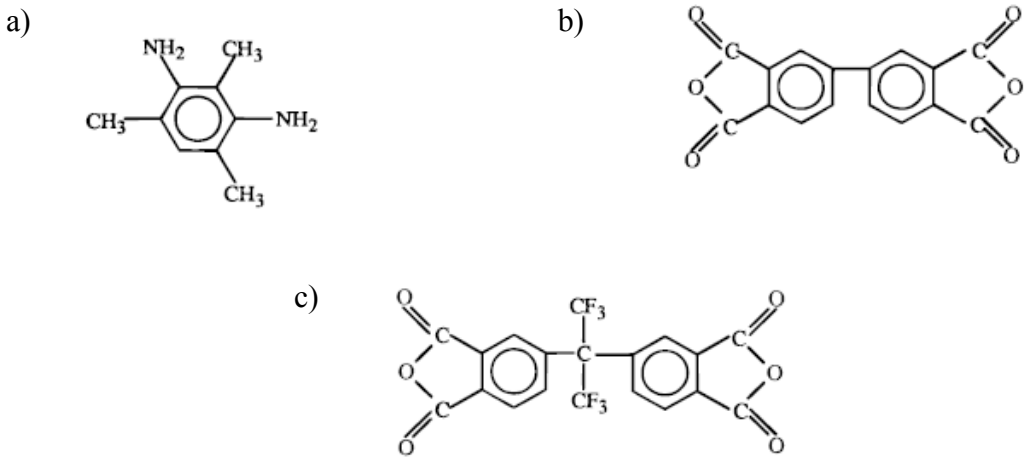

Figure 2.4 Monomers for polyimide used as the precursor for carbon molecular sieve membranes: (a) 2,4,6-trimethyl-1,3-phenylenediamine, (b) 3,4:3',4'-biphenyltetracarboxylic acid dianhydride, and (c) 5,5'-[2,2,2,-trifluoro-1-(trifluoromethyl)ethylidene]-bis-1,3-isobenzofurandione (Jones and Koros, 1994).

Steel and Koros, (2003) studied the pyrolysis temperature of Matrimid® polyimide from 500 to 800 ºC. As a result, a decrease in N_2 and O_2 permeability and increase in the O_2/N_2 selectivity after raising the pyrolysis temperature which finally changed the pore structure of polymer precursor to carbon molecular sieving material (CMS).

Centeno *et al*., (2004) studied the effect of pyrolysis temperature, heating rate, soak time and atmosphere on the membrane permeability and selectivity of phenolic resins-based CMS membrane. They reported that an increase of permeability could be done with lower pyrolysis temperature, lower heating rate, shorter soak time and inert atmosphere. However, this increment of permeability was reversibly proportional to its selectivity.

Anderson *et al*., (2008) studied the effect of pyrolysis temperature of polyfurfuryl alcohol (PFA) on performance as carbon membrane. Pyrolysis treatment at 300ºC was found sufficiently for the PFA precursor to degrade to a carbon solid. The increment of pyrolysis temperature resulted in the decrease of pore size but an increase to the membrane porosity as proven by the increment of gas permeance. The increment of the pyrolysis temperature from 300 to 600ºC has increased the O_2 and N_2 permeance which is attributed by the corresponding increase in porosity (Shiflett and Foley, 2000).

Burket *et al*., (2006) studied the pyrolysis temperature of polyfurfuryl alcohol (PFA) up to 600ºC. Micropores appear in the carbon as early as 300ºC along with a significant amount of mesopores. As the pyrolysis temperature is increased, microporosity is retained, but the mesoporosity disappears. At 600ºC, the material is microporous with a monodisperse pore size distribution centered at 4–5 ºA.

Mariwala and Foley, (1994) observed that the increasing of pyrolysis temperature caused the narrowing of pore size distribution due to the growth of the aromatic microdomains that subsequently led to an increase in porosity and consume the amorphous carbon. The permeation activation energies increased with the increase in membrane selectivity which correlates to an increase in pyrolysis temperature. The permeation energies of 4.1 and 5.2 kcal/mol for O_2 is obtained from pyrolysis temperature at 550 and 800ºC, respectively. Meanwhile, 6.1 and 6.6 kcal/mol can be obtained for N_2 at the previous pyrolysis temperature, respectively (Singh-Ghosal and Koros, 2000). This increment of activation energy was due to the shrinkage of contrictions in the channel responsible for the selectivity of a carbon structure when higher pyrolysis temperatures are applied (Steel and Koros, 2003).

Ali *et al*., (2011) prepared the activated carbon from PET wastes by a two-step physical activation method under N_2 and CO_2 atmosphere, respectively. In this study, an improved method was investigated to prepare high surface activated carbon. The characteristics of a typical commercial activated carbon were also measured and compared. It was found that the activated carbon had a well-developed micropore structure and BET surface area about 2010 m^2/g prepared from PET wastes at 975°C and 240 min holding time of activation stage and 800°C and 60 min holding time in carbonization stage . This carbon has 62% burn-off and 2.23 nm

average pore diameter with a total pore volume of 0.93 cm^3/g using N_2 adsorption at 77K. In addition, activated carbon produced was evaluated for its ability to remove phenol aqueous solution in a batch process. The results revealed that prepared activated carbon is expected to be an economical product for phenol removal for wastewater treatment.

Li *et al*., (2008) study the effects of different carbonization temperatures (400, 600, 800 and 1000°C) on characteristics of porosity in carbonized coconut shell char and activated carbon derived from carbonized coconut shell char with different activation times (30, 60, 90 and 120 min) at activation temperature of 900°C. The results showed that high temperature carbonized coconut shell char and activated carbon samples derived from high temperature carbonized coconut shell chars had higher BET surface area, total volume, micropore volume and yield as compared to those of low temperature carbonized coconut shell char and activated carbon derived from low temperature carbonized coconut shell char. The BET surface area, total volume and micropore volume of activated carbon prepared from char obtained at 1000°C with activation time of 120 min were 1926 m^2/g, 1.26 cm^3/g and 0.931 cm^3/g, respectively. From the results, it was concluded that we could produce high surface area activated carbons from coconut shells using physical activation (steam activation) by proper selections of carbonization temperature and activation time.

Mendez-Linan *et al*., (2010) studied the physical and chemical activation effect to polycarbonate (PC) derived carbon adsorbents for hydrogen and methane storage. The derived activated carbons are apparently microporous with a significant volume of narrow pore size, which make them efficient for the adsorption of both gases. PC was pyrolyzed at 950ºC for 1 hr at heating rate 5 ºC/min in inert atmosphere (100 cm^3/min N_2). A 26% carbon yield was obtained after the pyrolysis. The derived carbon was ground and sieved to 0.2-0.6 mm particle size. Sample was activated by physical activation at 950ºC for 1, 4 or 8 h in 100 cm^3/min CO_2. For the chemical activation, the char was mixed directly with the appropriate amount of KOH (powder) to obtain three different KOH/C weight ratios (1:1, 4:1, and 6:1). The mixture was treated at 600 and 800ºC for 1 h at inert atmosphere (100 cm^3/min N_2). Both activation methods are effective in tailoring a well-developed porous texture,

although chemical activation with KOH only generates micropores, while activation with CO_2 also generates some mesopores for long activation time.

Su and Lua, (2006) have shown that the effect of heating rate on gas permeability were unique. Their study showed that the increasing of heating rate from 0.5 to 4 ºC/min increased the He and CO_2 permeability but decreased the N_2 permeability and did not influence the O_2 permeability. However, the influence of heating rates was found negligible when the pyrolysis temperature reached 800ºC. Similar conclusion regarding the negligibility of heating rate at elevated pyrolysis temperature was also reported (Shao *et al*., 2005 and Foley *et al*., 1995).

Barbosa-Coutinho *et al*., 2003 showed that 1 ºC/min caused the severe crack on their hollow fiber carbon membrane and used 3 ºC/min instead. This phenomenon was believed to be due to the extended period of exposure to pyrolysis environment that introduced some graphite-like structure which was found fragile. Their work also showed that the heating rate has less dominating effect than pyrolysis temperature on the membrane structure during the pyrolysis.

2.5.2 Methane Adsorption

Hao *et al*.,(2013) studied the influence of oxygen group on methane adsorption onto coal. The bituminous coal from Yihai coal field in Qinghai province (China) used for starting material. It was modified by oxidation with H_2O_2, $(NH_4)_2S_2O_8$ and HNO_3 at room temperature. As a result, N_2 adsorption showed that specific surface area, total pore volume and micropore volume were decrease after oxidative modifications. X-ray photoelectron spectra data showed the oxygen functional group increase after oxidation with acid. The methane adsorption capacity measured by volumetric method at 303 K in pressure rang 0-5.3 MPa, data are correlated with Langmuir model and Dubinin-Astakho (D-A) model, found that the Dubinin-Astakho (D-A) model is the best fit. The result suggest that adsorption capacity decrease in oxidized samples as compared to unmodified sample and corresponded to its micropore volume. They found that coal with a higher amount of oxygen group and consequently with ales hydrophobic character, had lower methane adsorption capacity.

Feng *et al*., (2013) studied the role of oxygen containing group on coal surface influence for methane adsorption. Xingqing coal field in Qinghci China was modified with H_2SO_4, $(NH_4)_2S_2O_8$, and mixture of $H_2SO_4/(NH_4)_2S_2O_8$. Boehm titration was used to measure the quantities of oxygen containing group on coal surface, the result showed that after oxidation treatment by acid oxygen containing and carboxyl group on coal surface was increased. The methane adsorption isotherms were determined by volumetric method under pressure 4.0 MPa at temperature 298 K and the result fitted well by Langmuir model. The result showed that the adsorption capacity decreased after oxidation treatment because the increasing of oxygen containing groups. They concluded that oxygen group made the coal surface more hydrophilic and decrease amount of adsorption sites available for methane molecules.

Feng *et al*., (2014) studied methane adsorption behaviors of carbon spheres with nitrogen-containing groups which were prepared by urea, ammonia aqueous solution and NH_3 treatment. The adsorption characteristics of methane onto carbon spheres were measured at 298 K and pressure up to 5.0 MPa by volumetric method. The D-A model fitted the experimental data well. As a result, after treatments carbon spheres led to a decrease in adsorption capacity as compared with unmodified carbon sphere. They found that the surface properties, such as nitrogen-containing groups, were the sensitive factors. Meanwhile, a higher nitrogen content, especially a higher pyridine nitrogen content, provided more positive adsorptive sites for methane adsorption.

Vega *et al*., (2013) studied the effect of oxygen functional group of activated carbon (AC) on the adsorption of volatile sulphur compounds. Steam activated extruded RB3 carbon from Norit was used as raw material obtain a particle size between 63 and 212 μm. Chemical modifications were done by Nitric oxidation, ozone oxidation in gas phase and aqueous phase. The modifications with nitric acid and ozone oxidation caused changes in textural properties of AC as well as improve of oxgen-contaning group onto AC surface. The incorporation of oxygen group was higher with nitric acid than with ozone oxidation. The massive incorporation of oxygen functional group and the enrichment of hydroxyls internal surface of the carbon particles compensate the loss of porosity increasing the adsorption capacity of

ethyl mercaptan (ETM) and dimethyl sulphide (DMS). On the contrary, the studied oxidation treatments did not increase in the dimethyl disulphide (DMDS) adsorption.

Xinchenglu *et al*., (2012) studied the surface modification of coconut activated carbon by using chemical methods with different concentration of nitric acid oxidation at 25°C to produce oxygen functional group to enhance adsorption capacity of sodium and formaldehyde. The result from SEM showed morphology of activated carbon after oxidation some pore widening. The samples which oxidation by high concentration of nitric acid extent eroded and results in the pore blockage in the microporesbe consistent with the BET surface area and volume of activated carbon decreased. From Boehm method, the increasing of concentration of nitric acid, the amount of carboxylic group and phenolic group was increased. Fourier transform infrared spectroscopy (FTIR) was used to investigate functional groups. The presence of more -OH groups, -COOH groups in the oxidized ACs. Capacity of adsorption of sodium in oxidized carbon higher than unmodified ACs because the increasing of carboxylic and phenolic acid functionality in oxidized ACs, the adsorption capacity of formaldehyde increase from 11.5% to 24.2% after oxidation modified.

CHAPTER III
EXPERIMENTAL

3.1 Materials and Equipment

3.1.1 Materials and Chemicals

- Polycarbonate (PC; Wonder lite from CHI MIE corporation)
- Aniline (AR grade, Ani)
- Ammonium peroxydisulfate (AR grade, APS)
- Sulfuric acid (AR grade, H_2SO_4)
- Nitrogen gas (99.99% purity)
- Carbon dioxide gas (99.99% purity)
- Helium gas (99.99% purity)
- Methane gas (99.999% purity)

3.1.2 Equipment

- Quartz tube
- Electrical heater
- Fitting and valves
- Thermometer
- Centrifuge
- Volumetric apparatus for methane adsorption
- Data logger
- Vacuum pump
- Mass flow controller
- Pressure transducer
- BET surface area analyzer autosorb 1MP
- Oven
- Desiccators

3.2 Experimental Procedures

3.2.1 Preparation of Polymer Precursor

Polycarbonate (PC, Wonder lite) from CHI MIE corporation was used as received as polymer precursor. Polyaniline was prepared by oxidation and polymerization of 0.1 M Aniline and 0.1 M ammonium peroxydisulfate (APS) in 0.1 M sulfuric (H_2SO_4). After 2 days of polymerization, the reaction was complete. The sample was rinsed with de-ionized water and filtrated until neutrality was obtained. The sample was collected and dried in an oven at 70 °C overnight and then dried-sample was ground and sieved to 20-40 mesh size which was ready to use as polymer precursor.

3.2.2 Preparation of Carbon Molecular Sieve

10 g of polycarbonate or 2 g of polyaniline was weighed and carbonized at desired temperature (700, 800 or 900 °C) for 1 hr under inert nitrogen. Firstly, weighed polymer in the quartz tube reactor was flushed by inert nitrogen at flowrate 50 cm^3/min for 10 min (more than 3 times volume of reactor) before carbonization and activation step then heated the sample to desired temperature with a heating rate 5 °C/min.

After reaching the desired temperature, a sample was hold for 1 h carbonization under inert nitrogen atmosphere then switched the gas to CO_2 for activation with the same temperature that used in the carbonization step for 1 h.

After activation process, the sample was cooled to ambient temperature under inert nitrogen, then ground and sieved to 20-40 mesh size. Finally, the sample was dried in an oven at 110°C for 12 h and then kept in desiccators for the methane adsorption test and the characterization step.

The yield is calculate as follow:

$$yield(\%) = \frac{w_f}{w_i} \times 100\% \qquad (3.1)$$

Where: W_i is initial mass of the polymer precursor (polycarbonate or polyaniline, (g)

W_f is the mass of the sample after carbonization and activation, (g)

3.2.3 Characterization

BET surface area and pore analysis: BET surface area, micropore volume, total pore volume, and average pore diameter of the adsorbents were measured with the BET method on a Quantachrom/Autosorb1-MP instrument. Before analyzed, the adsorbents were removed the humidity on surface by out gassed under vacuum at 250 °C for approximately 15 hrs. After that, the adsorbent were analyzed by nitrogen adsorption isotherms at -196°C.

S_{BET} (BET surface area) was obtained from multiple point BET (Brunauer-Emmett-Teller) method which was derived from BET equation.

$$\frac{1}{W((P_0/P)-1)} = \frac{1}{W_m C} + \frac{C-1}{W_m C}\pi\frac{P}{P_0} \qquad (3.2)$$

Where: W = Weight of gas adsorbed at a relative pressure (P/P_0)

W_m= Weight of adsorbate forming a monolayer of surface coverage

C = A BET constant related to the energy of adsorption in the first adsorbed layer; its value is an indication of the magnitude of the adsorbent/adsorbate interactions

Micropore volume (V_{DR}) was obtained from DUBININ-RADUSHKEVICH (DR) method, which was calculated from the DR equation as followed,

$$V = V_0\left[-\left(\frac{A}{\beta E_0}\right)^2\right] \qquad (3.3)$$

Where: V = Volume of gas adsorption

V_0= Micropore volume

E_0= Characteristic energy of adsorption

A = Free adsorption energy

β = Affinity coefficient

Total pore volume was calculated from the amount of vapor adsorbed at a relative pressure close to unity, with the assumption that the pores were filled with liquid adsorbate.

Pore size distribution of micropores was calculated by HORVATH-KAWAZOE (HK) method from the low relative pressure region of the adsorption isotherm. Many pore size distribution methods are derived from the Kelvin equation which describes the phenomenon of capillary condensation. Some have questioned the reliability of the capillary condensation approach in the small confines of micropores. The HK method is derived independently from the Kelvin equation. The HK method expresses the adsorption potential function within slit-like micropores as a function of the effective pore width:

$$RT \ln\left(\frac{P}{P_0}\right) = K \frac{N_S A_S + N_A A_A}{\sigma^4 (\ell - d)} x \left[\frac{\sigma^4}{3\left(\ell - \frac{d}{2}\right)^3} - \frac{\sigma^{10}}{9\left(\ell - \frac{d}{2}\right)^9} - \frac{\sigma^4}{3\left(\frac{d}{2}\right)^3} + \frac{\sigma^{10}}{9\left(\frac{d}{2}\right)^9}\right] \quad (3.4)$$

where: K = Avogadro's number

N_S = number of atoms per unit area of adsorbent

$$A_S = \frac{6 mc^2 \alpha_s \alpha_A}{\frac{\alpha_s}{\chi_s} + \frac{\alpha_A}{\chi_A}}$$

N_A = number of molecules per unit area of adsorbate

m = mass of an electron

c = speed of light

α_s = polarizability of adsorbent

α_A = polarizability of adsorbate

χ_s = magnetic susceptibility of adsorbent

χ_A = magnetic susceptibility of adsorbate

$$A_A = \frac{3\,mc^2\,\alpha_A\,\chi_A}{2}$$

$(l\text{-}d_s)$ = effective pore width

$d = d_s + d_A$

d_s = diameter of adsorbent molecule

d_A = diameter of adsorbate molecule

l = distance between two layers of adsorbent

$\sigma = 0.858d/2$

By selecting effective pore widths in the micropore range, The following equation (3.5), a linear form of Eq. (3.3), can be used to calculate the corresponding relative pressures. From the adsorption isotherm, the amount of adsorption at each of these relative pressures is determined. Differentiation of weight (or volume) of gas adsorbed relative to the total uptake, W/W_0, with respect to the effective pore width yields a pore size distribution in the micropore range.

$$\log_{10} V = \log_{10}(V_0) - 2.303\left(\frac{RT}{\beta E_0}\right)^2 \log_{10}(P_0/P)^2 \qquad (3.5)$$

3.2.4 Methane Adsorption

3.2.4.1 Samples Preparation

The sample obtained from 3.2.2 was weighed for 1 g and put into the sample cell before placed in the volumetric apparatus.

3.2.4.2 Adsorption Experiment

The volumetric apparatus was used for study methane adsorption on carbon adsorbents. This apparatus consists of a sample holder, a vacuum pump, and pressure transducer. High purity grade of He (99.99% purity) was used to determine the volume of the apparatus including a buffer tank and a sample holder before methane adsorption was tested in each experiment. Ultra high purity grade methane (99.999% purity) was used in the adsorption study. The schematic diagram of volumetric apparatus for this research is shown in Figure 3.1.

A gas reservoir was a high pressure stainless steel reactor and the pressure regulator with 4,000 psig maximum limit was installed to control a gas flow rate into the system. A K-type thermocouple was used to measure the temperature of gas inside the reactor. The system pressure was measured by pressure transducer in the range of 0 to 3,000 psig with 0.13% error.

For each experiment, about 1 g of adsorbent was weighed and put into the sample holder then the adsorbent was degassed by using a rotary vacuum pump prior to the methane adsorption. The temperature was controlled at the desired temperature of 35 and 45ºC for each adsorption experiment with the pressure range of 0-800 psi. The pressures of gas were recorded before and after each gas expansion. The equilibrium adsorption can be indicated by the constant of final pressure.

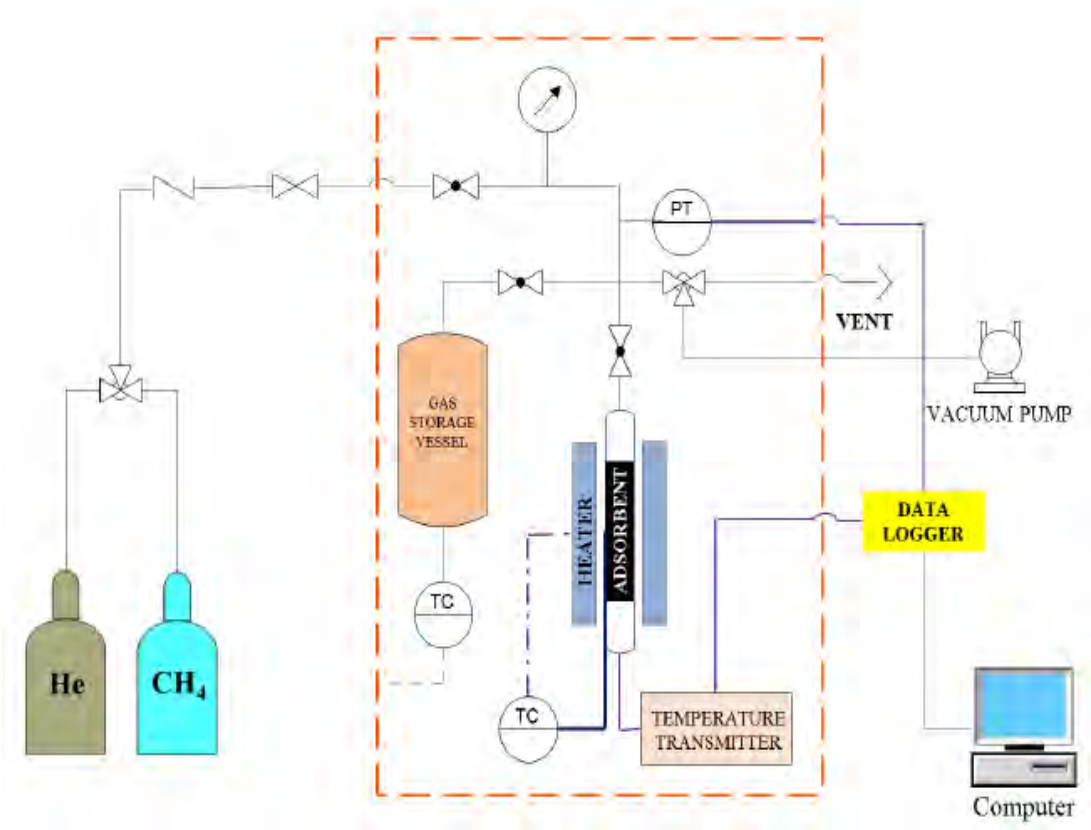

Figure 3.1 Schematic of the volumetric apparatus.

3.3 Adsorption and Calculation

3.3.1 Static Adsorption

The amount of methane adsorption was determined by using Eq. (3.6).

$$n_i = \frac{1}{W}\left(\frac{P_1(V_1+V_2)}{ZRT} - \frac{P_2(V_1+V_2)}{ZRT}\right) \qquad (3.6)$$

Where n = Mole of adsorbed CH_4 and CO_2 (mole)

P_1 = Pressure of the system before equilibrium (atm)

P_2 = Pressure of the system after equilibrium (atm)

V_1 = Volume of a manifold (cm^3)

V_2 = Volume of a cylinder with adsorbent (cm^3)

Z = Compressibility factor

R = 82.05 (cm^3atm/moleK)

T = Temperature of the sample (K)

W = Weight of adsorbent (g)

The pressure transducer was calibrated for each adsorption experiment. The vacuum pressure of -14.7 psi was used as the reference pressure. With this pressure, the relative was set to zero under vacuum condition.

3.3.1.1 Determination of the Sample Holder Volume using Helium

The volume of the sample holder was determined by helium expansion at 35 or 45°C, based on the assumption that no helium was adsorbed on the adsorbents. The pressures before and after each helium expansion were recorded. To calculate the volume of instrument after helium expansion, V_2, Ideal Gas Law was used as follows:

$$\frac{P_1V_1}{T_1} = \frac{P_2V_2}{T_2} \qquad (3.7)$$

Where: P_1 = Pressure of helium before helium expansion

V_1 = Volume of the system excluding volume of sample holder

T_1 = Temperature before helium expansion

P_2 = Pressure of helium after helium expansion

V_2 = Total system volume

= $V_1 + V_{sample\ holder}$

T_2 = Temperature after helium expansion

3.3.1.2 Determination of the Methane and Adsorption on Adsorbents

Determination of the methane adsorption was carried out at different constant temperatures (35 or 45 °C and pressure up to 800 psia). Temperature was heated up to the desired temperature at 35 or 45 °C. At desired pressure, methane was introduced from a high pressure cylinder into a sample holder. During the experiment, the time to reach the equilibrium of methane adsorption was within approximately 20 min. The methane pressures were recorded before and after each methane expansion.The ideal gas law and conservation of mass were also used for determining the amount of methane adsorbed on the adsorbents. The amounts of methane adsorbed by carbon adsorbents can be obtained by the following equation:

$$n_{ad} = n_{ad-1} + \frac{P_i V_1}{zRT_i} - \frac{P_{f-1} V_2}{zRT_{f-1}} - \frac{P_f (V_1 + V_2)}{zRT_f} \qquad (3.8)$$

Where: n_{ad} = Total amount methane adsorbed by carbon adsorbents (mole)

n_{ad-1} = Amount methane adsorbed at previous stage (mole)

P_i = Initial pressure of methane before methane expansion into the sample holder (psia)

P_{f-1} = Final pressure of methane after methane expansion into the sample holder in the previous stage (psia)

P_f = Final pressure of methane after methane expansion into the sample holder (psia)

V_1 = Volume of manifold excluding volume of sample holder (cm^3)

V_2 = Volume of the sample holder (cm^3)

Z = Compressibility factor of methane

T_i = Initial temperature of methane before methane expansion into the sample holder (K)

T_f = Final temperature of methane after methane expansion into the sample holder (K)

T_{f-1} = Final temperature of methane after methane expansion into the sample holder in the previous stage (K)

R = Gas constant, 82.0578 $atm \cdot cm^3/mol \cdot K$

CHAPTER IV
RESULTS AND DISCUSSION

4.1 Production of CMS

Two-step carbonization and activation was chosen for this research. The purpose of this process is to remain the carbonaceous carbon, eliminate the impurities to generate the pore in the carbon structure, and make a suitable material for adsorption process. 10 g of PC or 2 g of PANI was carbonized under inert nitrogen atmosphere in vertical quartz tube reactor at desired temperature (700 , 800 and 900°C) with the heating rate 5°C/min for 1 h. Carbonized polymer was continually activated by CO_2 at the same carbonization temperature for 1 h. The samples were weighed before and after the carbonization and activation to determine the yield of products. The results are reported in Table 4.1.

4.1.1 Effect of Polymer Precursor

Polymer precursor is related to the mass loss in carbonization and activation step. Their structure and bonding energy resulted to the proportional of gaseous and liquid yield that comes after reaching the required temperature. Volatile by-products such as H_2, H_2O, CO, CO_2, and smaller amounts of HCN, CH_4, and NH_3, depending on the polymer type, are released (Geiszler and Koros, 1996). The weight loss could reach as high as 70-95% (Lie and Hagg, 2006, Song *et al*., 2008). According to Table 4.1, it is obviously seen that the yield of CMS obtained from PANI is higher than those obtained from PC for all samples.

4.1.2 Effect of Carbonization and Activation Temperature

The carbonization and activation temperature is the significant parameter that affects to yield of the product. In Carbonization under nitrogen inert atmosphere, this process removes most of the heteroatoms in the polymer macromolecules carbon chain, leaving behind a crosslinked carbon with an amorphous microporous structure created by the evolution of gaseous products. It

also causes the rearrangement of the molecular structure of the polymeric precursor (Sedigh *et al*., 2000). The reaction that may occur under such condition to extract carbon atoms from the char structure is shown as follows:

$$C + CO_2 \longrightarrow 2CO;\ \Delta H = +159\ kJ/mol$$

This reaction is endothermic; therefore external energy is required to supply the high activation temperature which is almost above 800ºC (March *et al.*, 2006, Hayashi *et al.*, 2000). The result exhibits that the CMS yield is decreased with increasing carbonization and activation temperature. According to Table 4.1, yield of PC samples decreased from 31.1% to 29.4% while yield of PANI samples decreased from 57.4% to 50.6% as the carbonization and activation temperature increased (700 to 900°C).

Table 4.1 Yield of products after carbonization and activation at 700, 800 and 900°C

Precursor	Sample	Carbonization and activation temperature (ºC)	Yield (%)
Polycarbonate (PC)	PC_A700	700	31.1
	PC_A800	800	30.1
	PC_A900	900	29.4
Polyaniline (PANI)	PANI_A700	700	57.4
	PANI_A800	800	54.3
	PANI_A900	900	50.6

4.2 BET Surface Area and Pore Analysis

BET surface area and pore analysis of samples are summarized in Table 4.2. For PC, it is interesting to note that PC_A700 has both higher surface area and micropore volume than PC_A800 and PC_A900 which correspond to their methane adsorption capacity. As a result, the decreasing of surface area and pore volume was

affected by increasing of carbonization temperature that may lead to the destruction of some pores. However, an increase of the temperature was not effective in developing the microporosity of the sample. The results (PC-based CMS) show that a higher microporosity fraction (96%) was achieved at 700°C. Nevertheless, using activation temperature at 900°C (PC_A900) resulted in higher surface area and pore volume as compared to PC_A800. On the other hand, PANI_A900 provides the highest surface area and micropore volume in the PANI-series while PANI_A700 provides both higher surface area and micropore volume than PANI_A800. Furthermore, the results show that the higher carbonization and activation temperature, the smaller the pore sizes could be well achieved. Even though PC_A700 provide the highest fraction of micropore volume related to total pore volume which equals to 96%, its mean pore size (1.5 nm) is larger than PC_A800 and PC_A900 (1.3 and 1.1 nm, respectively). Meanwhile, the samples obtained from PANI (PANI_A700, PANI_A800 and PANI_A900) provide lower fractions of micropore volume related to their total pore volume (66.7%, 65.0% and 70.4%, respectively) while their mean pore sizes equal to 1.8, 1.6 and 1.5 nm, respectively. It obviously seen that mean pore sizes of PC-based CMS are quite smaller than those obtained from PANI-based CMS in each carbonization and activation temperature.

Table 4.2 The BET surface area and pore analysis of CMS obtained from polycarbonate and polyaniline by carbonization and activation at temperature 700, 800 and 900°C

Sample	BET Surface area, S_{BET} (m^2/g)	Micropore volume, V_{mic} (cc/g)	Total pore volume, V_t (cc/g)	V_{mic}/V_t (%)	Mean pore diameter (nm)
PC_A700	430.7	0.24	0.25	96.0	1.5
PC_A800	351.3	0.19	0.22	86.4	1.3
PC_A900	390.5	0.20	0.23	87.0	1.1
PANI_A700	180.6	0.16	0.24	66.7	1.8
PANI_A800	165.1	0.13	0.20	65.0	1.6
PANI_A900	283.0	0.19	0.27	70.4	1.5

The pore size distributions (PSD) of PC- and PANI-based CMS analyzed by Horvath-Kawazoe (HK) pore size analysis method for micropore are shown in Figure 4.1-4.2, respectively. Most of the pores are presented in the micropore region. Even though, their PSD are quite wider than common CMS but their PSD curves are different from activated carbon which generally consisted of higher proportion of mesopore. The sample; PC_A900, presents the narrowest PSD with mean pore size equals to 1.1 nm while the other samples; PC_A700 and PC_A800, present more wider PSD with mean pore size equal to 1.5 and 1.3 nm, respectively. Meanwhile PANI-based CMS provides more proportional of larger pore size with less micropore volume. As a result, the samples have a relatively narrow PSD as compare to activated carbon and also present the single pore size distributions corresponding to CMS characteristic.

Banisheykholeslami *et al*., (2015) prepared carbon molecular sieve (CMS) from broom corn stalk by carbon vapor deposition of methane. The base activated carbon (AC) was produced from the broom corn stalk using $ZnCl_2$ as the chemical activating agent. The comparison of PSD between activated carbon and CMS is illustated in Figure 4.3. The pore size distribution lies less than 10 nm which indicates the presence of both micropores and mesopores. They claim that the pore size distribution of the CMS sample was narrower and mainly composed of micropores compared to AC800. However, their sample consisted of higher proportion of mesopore (Blue zone in Figure 4.3), it still has been named as CMS. Furthermore, their CMS provides less ratio (60%) of micropore volume related to total pore volume (Table 4.3) as compared to micropore fraction of CMS in this study which provide the higher ratios of micropore up to 96%. Moreover, PC- and PANI-based CMS provide the narrower PSD that lies less than 4 nm. From these comparisons, it is believed that CMS may be successfully synthesized by carbonization and activation of PC and PANI precursor.

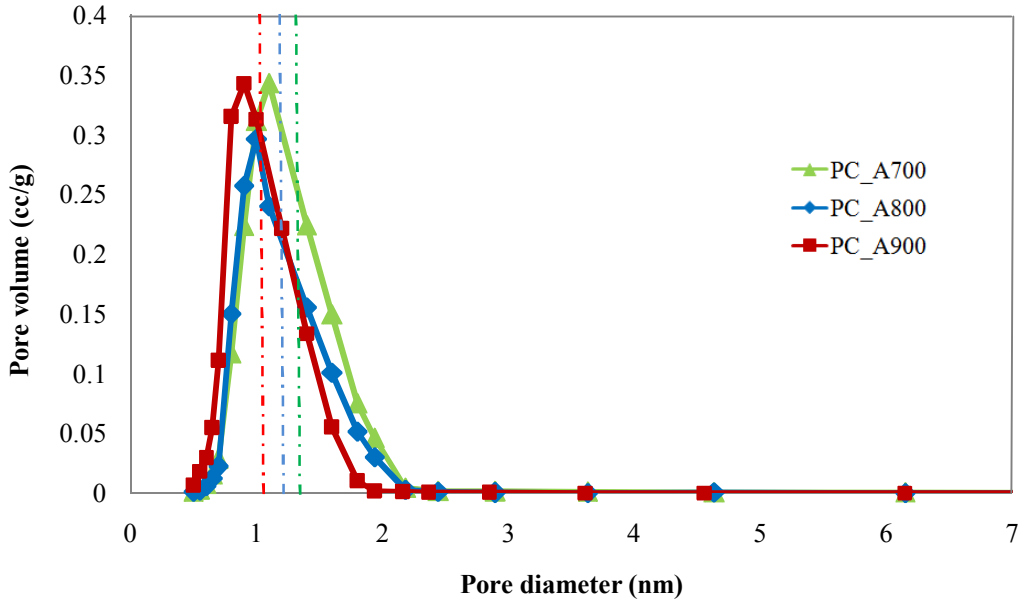

Figure 4.1 Pore size distribution of CMS obtained from polycarbonate by carbonization and activation at 700, 800 and 900°C.

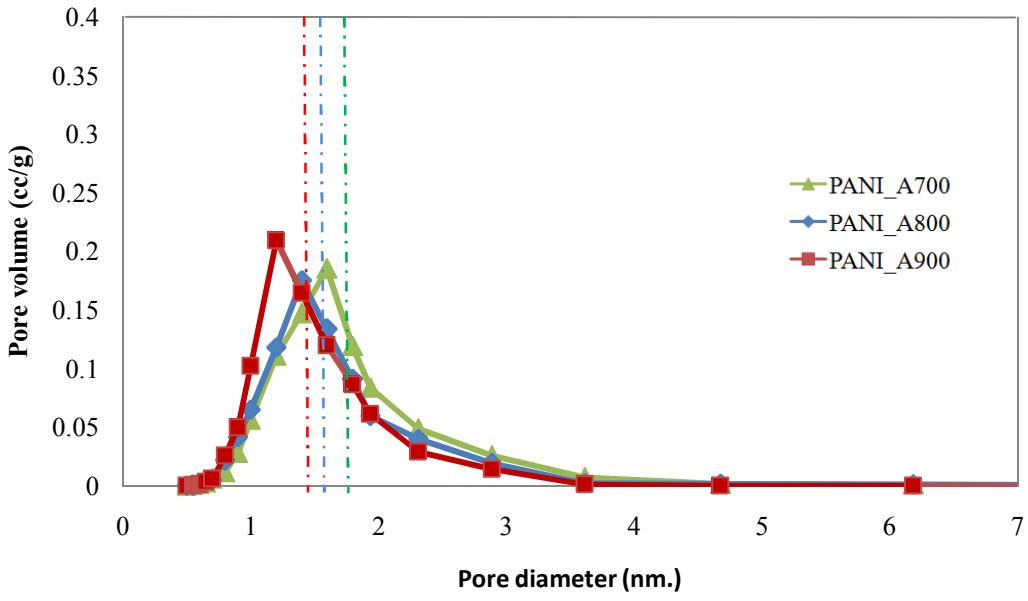

Figure 4.2 Pore size distribution of CMS obtained from polyaniline by carbonization and activation at 700, 800 and 900°C.

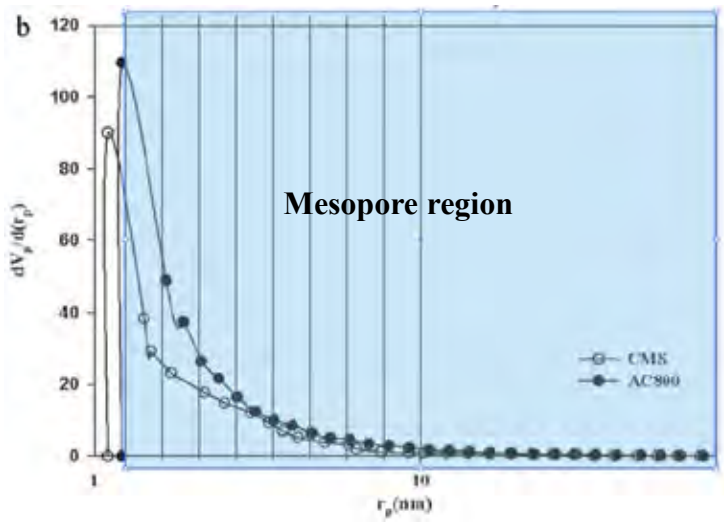

Figure 4.3 BJH pore size distribution of the produced ACs and CMS from broom corn stalk (Banisheykholeslami *et al*., 2015).

Table 4.3 The structural properties of adsorbents before and after CVD of methane (Banisheykholeslami *et al*., 2015)

Adsorbent	S_{BET} (m^2 /g)	Micropore Volume (cm^3/g)	Total pore volume (cm^3/g)	V_{mic}/V_t (%)	Mean pore diameter (nm)
AC800	1121.3	0.2251	0.5668	39.71	2.0219
AC950	1048	0.1772	0.5750	30.82	2.1946
CMS	815.6	0.1816	0.3001	60.53	1.4717

4.3 Methane Adsorption

The main objective of this section is to investigate methane adsorption capacity by volumetric apparatus. Figure 4.4 and 4.5 show the methane adsorption isotherm on CMS; PC_A700, PC_A800, PC_A900, PANI_A700, PANI_A800 and PANI_A900 at 35°C and 45°C with the pressure range from 0 to 800 psia. The methane adsorption isotherm was plotted between the methane adsorption capacity (mmol per gram of CMS) and equilibrium pressure (psia). As illustrated in Figure 4.4 and 4.5, the methane adsorption capacity is increased with increasing in the

pressure. From these results, it is interesting to note that PC_A700 has the highest methane adsorption capacity at both adsorption temperature of 35°C and 45°C. Meanwhile, the methane adsorption capacity of PANI at the temperature of 35°C and 45°C is increased with increasing carbonization and activation temperature. It can be explained and related to their BET surface area and pore analysis as shown in the previous section.

However, PANI_A800 performs the higher methane adsorption capacity than PANI_A700 even its surface area and micropore volume are less than that obtained from PANI_A700. It should be explained by the smaller micropore diameter that fits and supports multi-layer of adsorbed methane molecules. PANI_A800 may perform as Figure 4.6a while PANI_A700 may perform as Figure 4.6b. As a result, some vacant surfaces in the pores could not be occupied by the methane molecules which lead to less adsorption of methane.

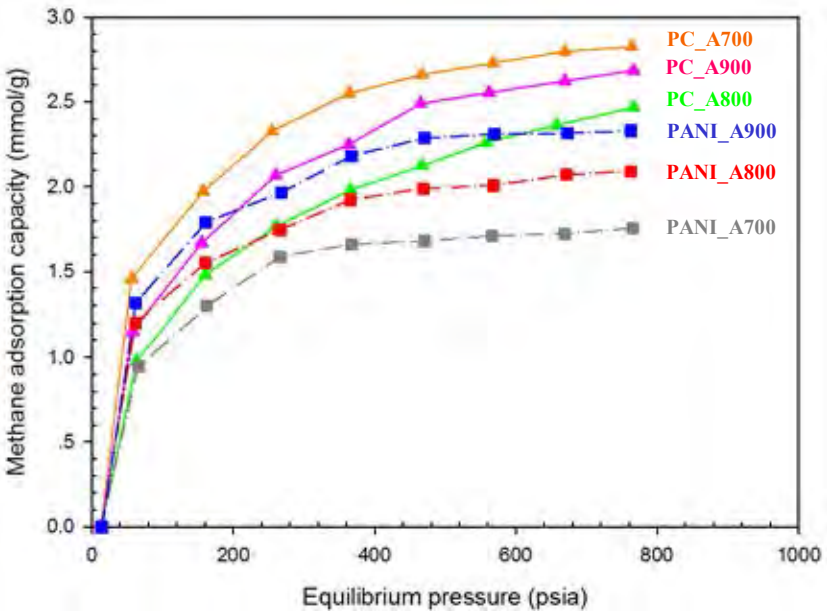

Figure 4.4 Methane adsorption at 35°C on CMS obtained from polycarbonate and polyaniline by carbonization and activation at temperature 700, 800 and 900°C.

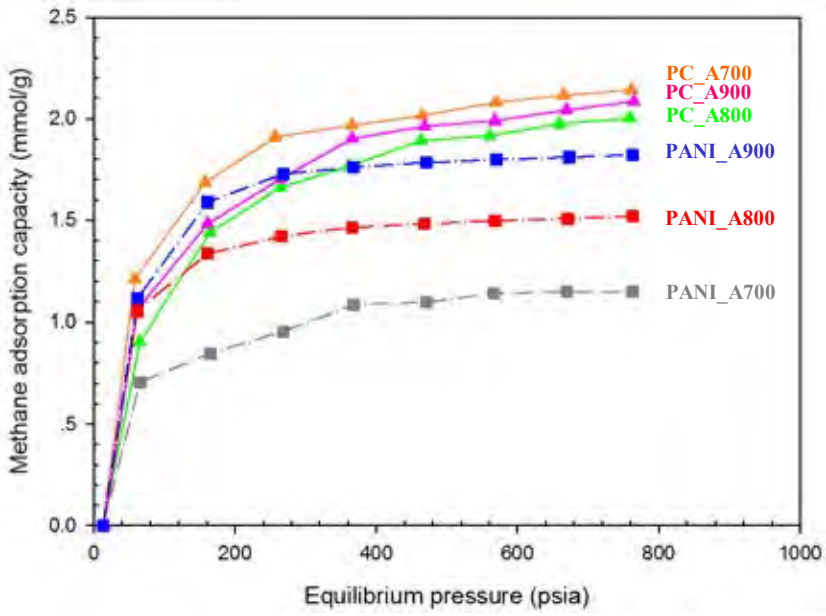

Figure 4.5 Methane adsorption at 45°C on CMS obtained from polycarbonate and polyaniline by carbonization and activation at temperature 700, 800 and 900°C.

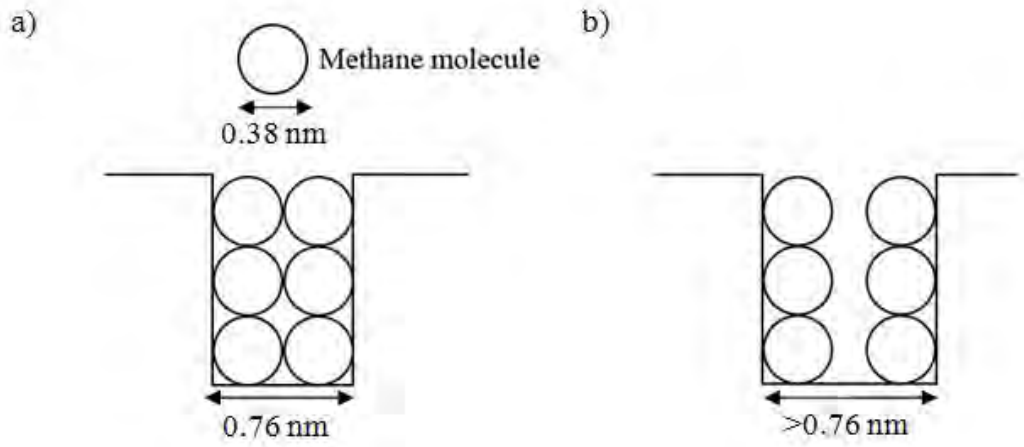

Figure 4.6 Methane molecules adsorbed on pores (Sudibandriyo, 2000).

According to Table 4.4, all samples provide the methane adsorption capacity at 35°C higher than that at 45°C. It obviously seen that the lower the adsorption temperature the higher the methane adsorption can be obtained due to the exothermic heat of adsorption (Wang *et al.*, 2010).

Table 4.4 The methane adsorption capacity (mmol/g) at 800 psi at 35 and 45°C

Sample	The methane adsorption capacity (mmol/g) at 800 psi	
	35°C	45°C
PC_A700	2.825	2.141
PC_A800	2.467	2.002
PC_A900	2.685	2.085
PANI_A700	1.755	1.147
PANI_A800	2.092	1.519
PANI_A900	2.330	1.821

From the previous work, Hirunstitporn, (2016) studied the methane adsorption on coconut shell-based activated carbon. Coconut shell that were heated up to final temperature at 300°C from Right Reactivation Public Company Limited were activated in the furnace at temperature 700, 800, 900 and 1000°C by using KOH or H_2SO_4 as oxidizing reagent. The samples after activation by using KOH are defined as ACX00K while the samples after activation by using H_2SO_4 are defined as ACX00H which X00 refer to activation temperature; 700, 800, 900 and 1000. The relations between the methane adsorption capacity at 800 psi and 35°C as a function of BET surface area and micropore volume, respectively are illustrated in Figure 4.7 and 4.8. In the previous work, all the samples perform that the increase of methane adsorption capacity corresponded to their BET surface area.

In addition, methane adsorption capacity per BET surface area of carbon adsorbents at 800 psi and 35°C is illustrated in Figure 4.9. As a result, PC-based CMS provides almost the same ratio of the methane adsorption capacity per BET surface area at different carbonization and activation temperature with the higher value (0.007 mmol CH_4/m^2) as compared to coconut shell-based activated carbon (0.005 mmol CH_4/m^2). However, an exceptional result from PANI-based CMS, each carbonization and activation temperature provides the different value of methane adsorption capacity per BET surface area. Furthermore, PANI_A800 exhibits the highest methane adsorption capacity per BET surface area (0.127 mmol/m^2) which

means that methane molecules are the most densely adsorbed on the surface of the pores of PANI_A800. It suggests that the methane adsorption capacity is not only depend on the BET surface area but also micropore volume and pore size diameter.

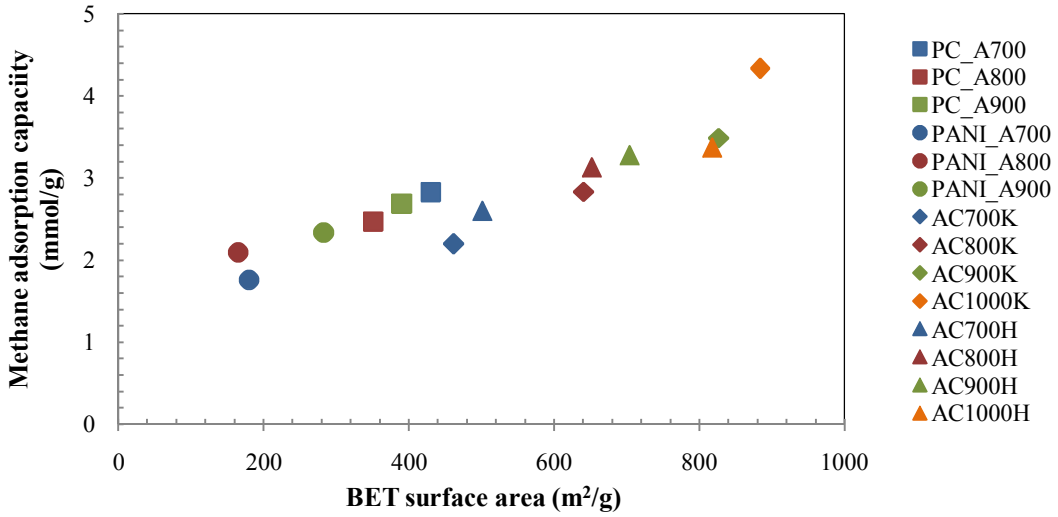

Figure 4.7 Methane adsorption (mmol/g) at 800 psi and 35°C as a function of BET surface area (m^2/g).

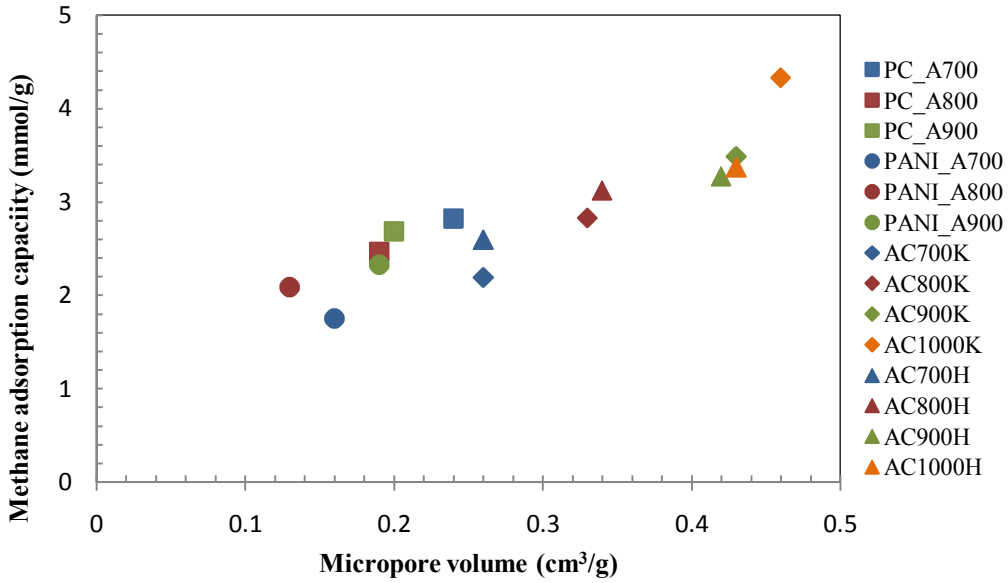

Figure 4.8 Methane adsorption (mmol/g) at 800 psi and 35°C as a function miccropore volume (cm^3/g).

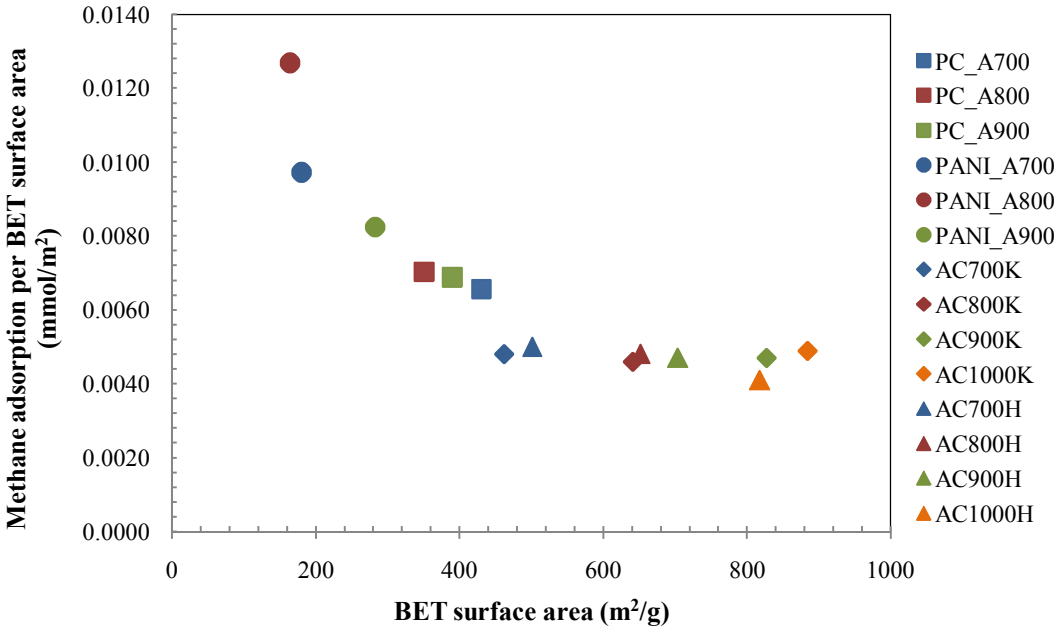

Figure 4.9 Methane adsorption per BET surface area (mmol/m^2) at 800 psi and 35°C with surface area (m^2/g).

Figure 4.10-4.11 show the relation of the methane adsorption capacity as a function of BET surface area and micropore volume at higher adsorption temperature (45°C), respectively. In addition, the methane adsorption capacity per BET surface area of carbon adsorbents at 800 psi and 45°C is illustrated in Figure 4.12. The results are in accordance with another adsorption temperature but all of these provide the lower performance in methane adsorption capacity. As a result, BET surface area and micropore volume are still mainly parameter of the adsorption capacity. Furthermore, an adsorption temperature is also important factor that affects to the adsorption behavior. It obviously seen that adsorption temperature has more effect on PANI-based CMS than PC-based CMS. Especially PANI_A700, their methane adsorption capacity per BET surface area is decreased from 0.0097 to 0.0064 mmol/m^2 which is decreased around 34%.

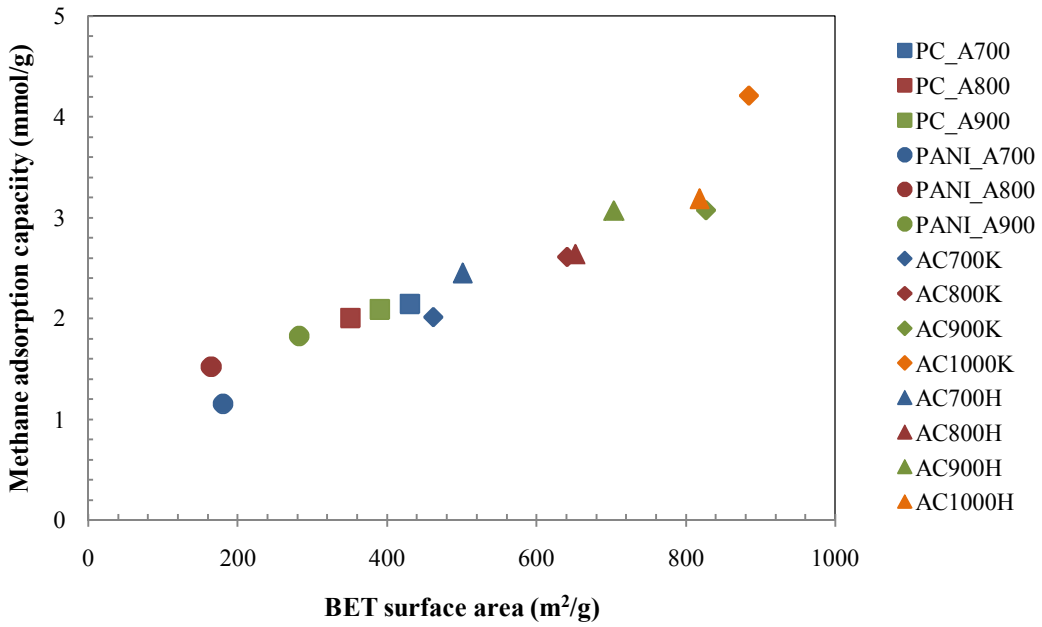

Figure 4.10 Methane adsorption (mmol/g) at 800 psi and 45°C as a function of BET surface area (m^2/g).

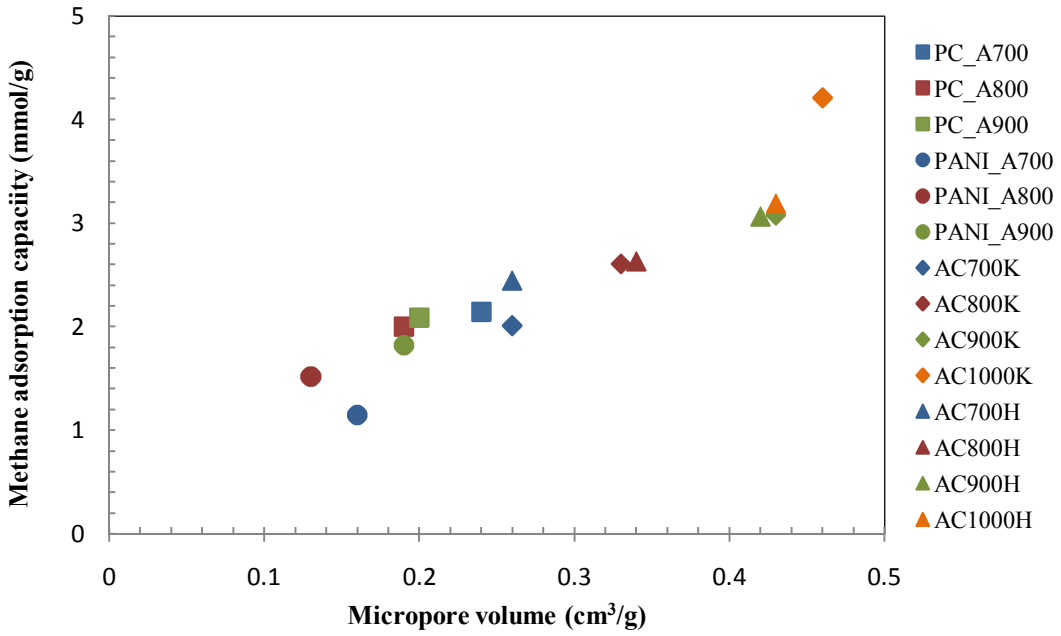

Figure 4.11 Methane adsorption (mmol/g) at 800 psi and 45°C as a function miccropore volume (cm^3/g).

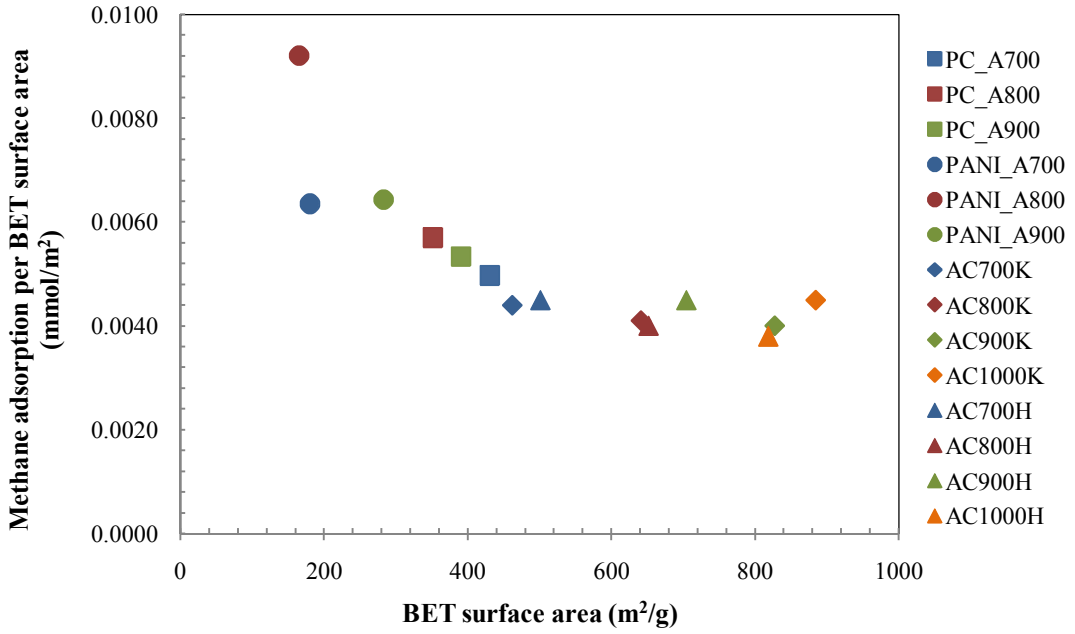

Figure 4.12 Methane adsorption per BET surface area (mmol/m^2) at 800 psi and 45°C with surface area (m^2/g).

The methane adsorption capacity per BET surface area (mmol/m^2) and the methane adsorption capacity per micropore volume (mmol/m^3) at 800 psi of carbon adsorbents at adsorption temperature of 35 and 45°C are summarized in Table 4.5. At low adsorption temperature, the methane adsorption capacity per BET surface area and the methane adsorption capacity per micropore volume are higher than that obtained at high adsorption temperature.

Moreover, PC- and PANI-based CMS can be performed in higher both adsorbed methane per area and adsorbed methane per volume. Accordingly, in this point of view, these CMS are more effective in methane adsorption than activated carbon owing to some unique characteristics of their pores that could not be acquired by activated carbon. Therefore, their surface area and micropore volume need to be increased on the condition that most of their pore sizes should be suitable for adsorbed methane molecules like two-layer adsorption to perform as competitive adsorbent for methane storage.

Table 4.5 The methane adsorption capacity per BET surface area (mmol/m^2) and the methane adsorption capacity per micropore volume (mmol/m^3) at 800 psi and different activation temperature

Sample	The methane adsorption capacity per BET surface area capacity (mmol/m^2) at 800 psi		The methane adsorption capacity per micropore volume (mmol/m^3) at 800 psi	
	35 ºC	45 ºC	35 ºC	45 ºC
PC_A700	0.0066	0.0050	11.770	8.921
PC_A800	0.0070	0.0057	12.984	10.537
PC_A900	0.0069	0.0053	13.425	10.425
PANI_A700	0.0097	0.0064	10.969	7.169
PANI_A800	0.0127	0.0092	12.306	8.935
PANI_A900	0.0082	0.0064	12.263	9.584
AC1000K	0.0049	0.0045	8.840	8.014
AC1000H	0.0041	0.0038	7.172	6.490
AC900K	0.0047	0.0040	8.112	7.543
AC900H	0.0047	0.0045	7.798	7.385
AC800K	0.0046	0.0041	8.576	7.670
AC800H	0.0048	0.0040	8.230	7.024
AC700K	0.0048	0.0044	8.131	6.933
AC700H	0.0050	0.0045	8.375	8.014

CHAPTER V
CONCLUSIONS AND RECOMMENDATIONS

5.1 Conclusions

Polycarbonate and polyaniline were used as a raw material to produce the carbon molecular sieve by carbonization and activation. The samples were carbonized under nitrogen inert atmosphere and then activated by physical activation under carbon dioxide. Type of polymer precursor significantly affected to yield of product and characteristics that related to the adsorption capacity in gas storage application. However, other factors are also important to produce the carbon molecular sieve. The carbonization and activation temperature mainly affect to yield and characteristics of product. As expected, the yield of CMS was decreased as the carbonization and activation temperature increased. Moreover, the results showed that, the higher the carbonization and activation temperature was utilized, the lower the pore size was achieved. In addition, the activation temperature can narrow down the pore size distribution. As a result, the samples have a relatively narrow PSD as compare to activated carbon and also present the single pore size distributions corresponding to CMS characteristic.

The highest methane adsorption capacity at 35°C of CMS derived from PC is 2.82 mmol CH_4/g of CMS. The methane adsorption of the PC-based CMS is higher than those obtained from PANI at the same carbonization and activation temperature. Furthermore, it is interesting to note that the CMS derived from 700°C carbonization and activation of PC performs a higher methane adsorption capacity than those obtained from 800 and 900°C due to a higher surface area and higher amount of micropore volume. However, the methane adsorption capacity does not depend only on BET surface area and micropore volume, but also depend on the pore size of CMS. Therefore, the physical properties of CMS, including the BET surface area, micropore volume, total pore volume, and pore size diameter, play an important role in the adsorption of methane. Thus, porous material such as CMS could increase the capacity of methane storage in the CNG tank.

5.2 Recommendations

To increase the capacity of methane adsorption, the CMS should be increased the surface area by improving porous structure. There are several methods to be achieved to perform a high surface area materials such as finding a suitable polymer precursor, optimizing the carbonization and activation temperature and adjusting the activation time or heating rate in the carbonization and activation step.

REFERENCES

Abhishankar, K. (2011) Adsorption of methane on activated carbon by volumetric method. M.S.Thesis, National Institute of Technology, Rourkela, India.

Ahmadpour, A., Okhovat, A., and Mahboub, M.D. (2013) Pore size distribution analysis of activated carbons prepared from coconut shell using methane adsorption data. Journal of Physics and Chemistry of Solids, 74(6), 886-891.

Alcaniz-Monge, J., De la Casa-Lillo, M.A., Cazorla-Amorós, D., and Linares-Solano, A. (2002) Advances in the study of methane storage in porous carbonaceous materials. Fuel, 81(14), 1777-1803.

Ali, E., Tahereh, K., and Mansooreh, S. (2011) Preparation of high surface area activated carbon from polyethylene terephthalate (PET) waste by physical activation. Journal of Chemical and Environmental Sciences, 15 (2), 433-437.

Allwar, A. (2012) Characteristics of pore structures and surface chemistry of activated carbons by physisorption, FTIR and Boehm Methods. Journal of Applied Sciences, 2, 9-15.

Alslaibi, T.M., Abustan, I., Ahmad, M.A., and Foul, A.A. (2013) A review: production of activated carbon from agricultural byproducts via conventional and microwave heating. Journal of Chemical Technology and Biotechnology, 88(7), 1183-1190.

Anderson, C.J., Pas, S.J., Arora, G., and Kentish, S.E. (2008) Effect of pyrolysis temperature and operating temperature on the performance of nanoporous carbon membranes. Journal of Membrane Science, 332, 19-27.

Bagheri, N. and Abedi, J. (2011) Adsorption of methane on corn cobs based activated carbon. Chemical Engineering Research and Design, 89(10), 2038-2043.

Balek, V. and Koranyi, A.D. (1990) Diagnostics of structural alterations in coal: porosity changes with pyrolysis temperature. Fuel, 69(12), 1502-1506.

Baker, F.S., Miller, C.E., Repic, A.J., and Tolles, E.D. (1992) Activated carbon. Kirk Othmer Encyclopedia of Chemical Technology, 4, 1015-1037.

Barbosa-Coutinho, E., Salim,V.M.M., and Borges, C.P. (2003) Preparation of carbon hollow fiber membranes by pyrolysis of polyetherimide. Carbon, 41, 1707-1714.

Bastos-Neto, M., Canabrava, D.V., Torres, A.E.B., Rodriguez-Castellón, E., Jiménez-López, A., Azevedo, D.C.S., and Cavalcante, C.L. (2007) Effects of textural and surface characteristics of microporous activated carbons on the methane adsorption capacity at high pressures. Applied Surface Science, 253, 5721–5725.

Burket, C.L., Rajagopalan, R., Marencic, A.P., Dronvajjala, K., and Foley, H.C. (2006) Genesis of porosity in polyfurfuryl alcohol derived nanoporous carbon. Carbon, 44, 2957-2963.

Celzard, A. and Fierro, V. (2005) Preparing a suitable material designed for methane storage: a comprehensive report. Energy & fuels, 19(2), 573-583.

Centeno, T.A., Vilas, J.L., and Fuertes, A.B. (2004) Efects of phenolic resin pyrolysis conditions on carbon membrane performance for gas separation. Journal of Membrane Science, 228, 45-54.

Chandra, T.C., Mirna, M.M., Sudaryanto, Y., and Ismadji, S. (2007) Adsorption of basic dye onto activated carbon prepared from durian shell: Studies of adsorption equilibrium and kinetics. Chemical Engineering Journal, 127(1-3), 121-129.

Dai, X.D., Liu, X.M., Zhao, G., Qian, L., Qiao, K., and Yan, Z.F. (2008) Treatment of activated carbon for methane storage. Asia-Pacific Journal of Chemical Engineering, 3(3), 292-297.

Delavar, M., Ghoreyshi, A.A., Jahanshahi, M., and Irannejad, M. (2010) Experimental evaluation of methane adsorption on granular activated carbon (GAC) and determination of model isotherm. World Academy of Science, Engineering and Technology, 62, 47-50.

Derylo-Marczewska, A., Buczek, B., and Swiatkowski, A. (2010) Effect of oxygen surface groups on adsorption of benzene derivatives from aqueous solutions onto active carbon samples. Applied Surface Science, 257, 9466-9472.

Dombrowski, R.J., Lastoskie, C.M., and Hyduke, D.R. (2001) The Horvath–Kawazoe method revisited. Colloids and Surfaces A: Physicochemical and Engineering Aspects, 187, 23-39.

El-Hendawy, A.A. (2003) Influence of HNO_3 oxidation on the structured and adsorptive properties of corncobs activated carbon. Carbon, 41, 713-722.

Farzad, S., Taghikhani, V., Ghotbi, C., Aminshahidi, B., and Lay, E.N. (2007) Experimental and theoretical study of the effect of moisture on methane adsorption and desorption by activated carbon at 273.5 K. Journal of Natural Gas Chemistry, 16(1), 22-30.

Farzaneh-Gord, M., Deymi-Dashtebayaz, M., and Rahbari, H.R. (2011) Studying effects of storage types on performance of CNG filling stations. Journal of Natural Gas Science and Engineering, 3(1), 334-340.

Feng, Y., Yang, W., Liu, D., and Chu, W. (2013) Surface modification of bituminous coal and its effects on methane adsorption. Chinese Journal of Chemistry, 31(8), 1102-1108.

Feng, Y., Yang, W., Wang, N., Chu, W., and Liu, D. (2014) Effect of nitrogen-containing groups on methane adsorption behaviors of carbon spheres. Journal of Analytical and Applied Pyrolysis, 107, 204-210.

Foley, H.C. (1995) Carbogenic molecular sieve: Synthesis, properties and applications. Microporous Materials, 4, 407-433.

Gándara, F., Furukawa, H., Lee, S., and Yaghi, O. M. (2014) High methane storage capacity in aluminum metal–organic frameworks. Journal of the American Chemical Society, 136(14), 5271-5274.

Geiszler, V.C. and Koros, W.J. (1996) Effects of polyimide pyrolysis conditions on carbon molecular sieve membrane properties. Industrial & Engineering Chemistry Research, 35, 2999-3003.

Hao, S.X., Wen, J., Yu, X.P., and Chu, W. (2013) Effect of the surface oxygen groups on methane adsorption on coals. Applied Surface Science, 264, 433–442.

Hayashi, J., Kazehaya, A., Muroyama, K., Watkinson, A. (2000) Preparation of activated carbon from lignin by chemical activation. Carbon, 38, 1873–1878.

Hirunstitporn, T. (2016) Methane adsorption by activated porous carbons derived from coconut shell. M.S. Thesis, The Petroleum and Petrochemical College, Chulalongkorn University, Bangkok, Thailand.

Iijima, S. (2002) Carbon nanotubes: past, present, and future. Physica B: Condensed Matter, 323, 1–5.

Jones, C.W. and Koros, W.J. (1994) Carbon molecular sieve gas separation membranes - I. Preparation and characterization based on polyimide precursors. Carbon, 32, 1419-1425.

Kumar, S., Kwon, H.T., Choi, K.H., Lim, W., Cho, J.H., Tak, K., and Moon, I. (2011) LNG: An eco-friendly cryogenic fuel for sustainable development. Applied Energy, 88(12), 4264-4273.

Le, V.T., Ngo, C.L., Le, Q.T., Ngo, T.T., Nguyen, D.N., and Vu, M.T. (2013) Surface modification and functionalization of carbon nanotube with some organic compounds. Advances in Natural Sciences: Nanoscience and Nanotechnology, 4(3), 1-5.

Li, L., Liu, S., and Liu, J. (2011) Surface modification of coconut shell based activated carbon for the improvement of hydrophobic VOC removal. Journal of Hazardous Materials, 192, 683-690.

Li, W., Yang, K., Peng, J., Zhang, L., Guo, S., and Xia, H. (2008) Effects of carbonization temperatures on characteristics of porosity in coconut shell chars and activated carbons derived from carbonized coconut shell chars. Industrial Crops and Products, 28(2), 190-198.

Lie, J.V. and Hagg, M.B. (2006) Carbon membranes from cellulose: Synthesis, performance and regeneration. Journal of Membrane Science, 284, 79-86.

Lozano-Castello, D., Alcaniz-Monge, J., Casa-Lillo, M.A., Cazorla-Amoro, D., and Linares-Solano, A. (2002a) Advances in the study of methane storage in porous carbonaceous materials. Fuel, 81, 1777–1803.

Lozano-Castello, D., Cazorla-Amoros, D., Linares-Solano, A., and Quinn, D.F. (2002b) Influence of pore size distribution on methane storage at relatively low pressure: preparation of activated carbon with optimum pore size. Carbon, 40(7), 989-1002.

Lozano-Castello, D., Cazorla-Amoros, D., and Linares-Solano, A. (2002c) Powdered activated carbons and activated carbon fibers for methane storage: a comparative study. Energy and Fuels, 16(5), 1321-1328.

Makal, T.A., Li, J.R., Lu, W., and Zhou, H.C. (2012) Methane storage in advanced porous materials. Chemical Society Reviews, 41(23), 7761-7779.

Mariwala, R.K. and Foley, H.C. (1994) Evolution of ultramicroporous adsorptive structure in poly(furfuryl alcohol)-derived carbogenic molecular sieves. Industrial & Engineering Chemistry Research, 33, 607-615.

Marsh, H. and Rodriguez-Reinoso, F. (2006) Activated Carbon. Amsterdam: Elsevier.

Masel, R.I., (1996) Principles of Adsorption and Reaction on Solid Surface, New York: John Wiley.

Mattson, J.S. and Mark H.B. (1971) Activated carbon, New York: Marcel Dekker.

Mendez-Linan, L., Lopez-Garzon, F.J., Domingo-Garcia, M., and Perez-Mendoza, M. (2010) Carbon adsorbents from polycarbonate pyrolysis char residue: Hydrogen and methane storage capacities. Energy and Fuels, 24, 3394–3400.

Menon, V.C., and Komarneni, S. (1998) Porous adsorbents for vehicular natural gas storage: a review. Journal of Porous Materials, 5(1), 43-58.

Mohamed, A.R., Mohammadi, M., and Darzi, G.N. (2010) Preparation of carbon molecular sieve from lignocellulosic biomass: A review. Renewable and Sustainable Energy Reviews, 14(6), 1591-1599.

Narges, B. and Abedi, J. (2011) Adsorption of methane on corn cobs based activated carbon. Chemical Engineering Research and Design, 89(10), 2038-2043.

Najibi, H., Chapoy, A., and Tohidi, B. (2008) Methane/natural gas storage and delivered capacity for activated carbons in dry and wet conditions. Fuel, 87(1), 7-13.

Patel, A. (2000) Hydrogen storage in carbon nanotubes. M.S. Thesis, University of Oklahoma, Norman, USA.

Pragya, P., Sripal, S., and Maheshkumar, Y. (2013) Preparation and study of properties of activated carbon produced from agricultural and industrial waste shells. Research Journal of Chemical Sciences, 3(12), 12-15.

Rafsanjani, H.H., Kamandari, H., and Najjarzadeh, H. (2013) Study on pore and surface development of activated carbon produced from Iranian coal in a rotary kiln reactor. Iranian Journal of Chemical Engineering, 10(3), 27-38.

Rıos-Mercado, R.Z. and Borraz-Sánchez, C. (2014) Optimization problems in natural gas transportation systems: A State-of-the-Art Review. Applied Energy, 147, 536-555.

Sedigh, M.G., Jahangiri, M., Liu, P.K.T., Sahimi, M., and Tsotsis, T.T. (2000) Structural characterization of polyetherimide-based carbon molecular sieve membranes. AIChE Journal, 46, 2245-2255.

Shabanzadeh, A. (2012) Production of activated carbon within the indirect gasification process. M.S. Thesis, Chalmers university of technology, Gothenburg, Sweden.

Shafawati, S.N. and Siddiquee, S. (2013) Composting of oil palm fibres and Trichoderma spp. as the biological control agent: A review. International Biodeterioration & Biodegradation, 85, 243-253.

Shao, L. Chung, T.S., and Pramoda, K.P. (2005) The evolution of physicochemical and transport properties of 6FDA-durene toward carbon membranes; from polymer, intermediate to carbon. Microporous and Mesoporous Materials, 84, 59-68.

Shiflett, M.B. and Foley, H.C. (2000) On the preparation of supported nanoporous carbon membranes. Journal of Membrane Science, 179, 275-282.

Sing, K.S. (1985) Reporting physisorption data for gas/solid systems with special reference to the determination of surface area and porosity. Pure and Applied Chemistry, 57(4), 603-619.

Singh-Ghosal, A. and Koros, W.J. (2000) Air separation properties of flat sheet homogeneous pyrolytic carbon membranes. Journal of Membrane Science, 174, 177-188.

Solar, C., Blanco, A.G., Vallone, A., and Sapag, K. (2010) Adsorption of methane in porous materials as the basis for the storage of natural gas. Natural Gas, 10, 205-244.

Soleimani, M. and Kaghazchi, T. (2008) Activated hard shell of apricot stones: A promising adsorbent in gold recovery. Chinese Journal of Chemical Engineering, 16(1), 112-118.

Song, C., Wang, T., Qui, J., Cao,Y., and Cai, T. (2008) Effects of carbonization conditions on the properties of coal-based microfiltration carbon membranes. Journal of Porous Materials, 15, 1-6.

Steel, K.M., and Koros, W.J. (2003) Investigation of porosity of carbon materials and related effects on gas separation properties. Carbon, 41, 253-266.

Su, J. and Lua, A.C. (2006) Effects of carbonization atmosphere on the structural characteristics and transport properties of carbon membranes prepared from Kapton® polyimide. Journal of Membrane Science, 305, 263-270.

Suda, H.and Haraya, K. (1997) Gas Permeation through micropores of carbon molecular sieve membranes derived from kapton polyimide. Journal of Physical Chemistry B, 101, 3988-3994.

Sudibandriyo, M. (2011) High pressure adsorption of methane and hydrogen at 25°C on activated carbons prepared from coal and coconut shell. International Journal of Engineering & Technology, 11(2), 79-85.

Sun, J., Brady, T.A., Rood, M.J., Rostam-Abadi, M., and Lizzio, A.A. (1996) Absorbed natural gas storage with activated carbon. Preprints of papers american chemical society division fuel chemistry, 41, 246-250.

Uysal, T., Duman, G., Onal, Y., Yasa, I., and Yanik, J. (2014) Production of activated carbon and fungicidal oil from peach stone by two-stage process. Journal of Analytical and Applied Pyrolysis, 108, 47-55.

Vega, E., Lemus, J., Anfruns, A., Gonzalez-Olmos, R., Palomar, J., and Martin, M.J. (2013) Adsorption of volatile sulphur compounds onto modified activated carbons: Effect of oxygen functional groups. Journal of Hazardous Materials, 258-259, 77-83.

Wang, Y.X., Liu, B.S., and Zheng, C. (2010) Preparation and adsorption properties of corncob-derived activated carbon with high surface area. Journal of Chemical and Engineering Data, 55(11), 4669-4676.

Yang, R.T., (1987) Gas Separation by Adsorption Process. New York: Butterworth.

APPENDIX

The Amount of Methane Adsorbed on Each Adsorbent at Temperature of 35ºC and 45ºC

Table 1 The amount of methane adsorption on PC_A700 at 35 °C

Equilibrium pressure (psi)	Methane adsorption (mmol/g)
13.13	0.000
56.26	1.4593
157.51	1.9712
255.01	2.3276
363.76	2.5508
466.88	2.6599
568.13	2.7294
669.38	2.7971
763.13	2.8247

Table 2 The amount of methane adsorption on PC_A800 at 35 °C

Equilibrium pressure (psi)	Methane adsorption (mmol/g)
13.13	0.000
63.76	0.9787
161.26	1.4825
260.63	1.7647
365.63	1.9806
466.88	2.1224
558.76	2.2608
658.13	2.3637
763.13	2.4673

Table 3 The amount of methane adsorption on PC_A900 at 35 °C

Equilibrium pressure (psi)	Methane adsorption (mmol/g)
13.13	0.000
58.13	1.154
155.63	1.668
260.63	2.068
363.76	2.250
465.01	2.490
562.51	2.556
669.38	2.623
763.13	2.685

Table 4 The amount of methane adsorption on PANI_A700 at 35 °C

Equilibrium pressure (psi)	Methane adsorption (mmol/g)
13.13	0.000
65.63	0.707
165.01	0.848
268.13	0.957
367.51	1.083
470.63	1.095
566.26	1.140
669.38	1.145
763.13	1.147

Table 5 The amount of methane adsorption on PANI_A800 at 35 °C

Equilibrium pressure (psi)	Methane adsorption (mmol/g)
13.13	0.000
61.88	1.057
161.26	1.335
266.26	1.421
365.63	1.464
468.76	1.482
568.13	1.498
671.26	1.508
763.13	1.519

Table 6 The amount of methane adsorption on PANI_A900 at 35 °C

Equilibrium pressure (psi)	Methane adsorption (mmol/g)
13.13	0.000
61.88	1.114
161.25	1.589
268.13	1.768
367.5	1.901
470.63	1.989
570	2.010
673.13	2.036
763.13	2.040

Table 7 The amount of methane adsorption on PC_A700 at 45 °C

Equilibrium pressure (psi)	Methane adsorption (mmol/g)
13.13	0.000
58.13	1.210
157.51	1.686
256.88	1.910
365.63	1.967
465.01	2.015
570.01	2.081
665.63	2.116
763.13	2.141

Table 8 The amount of methane adsorption on PC_A800 at 45 °C

Equilibrium pressure (psi)	Methane adsorption (mmol/g)
13.13	0.000
65.63	0.904
165.01	1.440
264.38	1.661
361.88	1.766
463.13	1.892
560.63	1.915
660.01	1.975
763.13	2.002

Table 9 The amount of methane adsorption on PC_A900 at 45 °C

Equilibrium pressure (psi)	Methane adsorption (mmol/g)
13.13	0.000
61.88	1.060
161.25	1.482
264.38	1.704
365.63	1.901
468.75	1.963
568.13	1.991
669.38	2.043
763.13	2.085

Table 10 The amount of methane adsorption on PANI_A700 at 45 °C

Equilibrium pressure (psi)	Methane adsorption (mmol/g)
13.13	0.000
65.63	0.707
165.01	0.848
268.13	0.957
367.51	1.083
470.63	1.095
566.26	1.140
669.38	1.147
763.13	1.147

Table 11 The amount of methane adsorption on PANI_A800 at 45 °C

Equilibrium pressure (psi)	Methane adsorption (mmol/g)
13.13	0.000
61.88	1.057
161.26	1.335
266.26	1.421
365.63	1.464
468.76	1.482
568.13	1.498
671.26	1.508
763.13	1.519

Table 12 The amount of methane adsorption on PANI_A900 at 45 °C

Equilibrium pressure (psi)	Methane adsorption (mmol/g)
13.13	0.000
61.88	1.114
161.25	1.589
268.13	1.728
367.5	1.760
470.63	1.785
570.00	1.797
673.13	1.811
763.13	1.821

Table 13 The amount of methane adsorption on CAC at 35 °C

Equilibrium pressure (psi)	Methane adsorption (mmol/g)
13.13	0.000
48.76	2.089
142.51	3.482
249.38	3.937
358.13	4.228
463.13	4.347
564.38	4.582
661.88	4.818
763.13	4.874

CURRICULUM VITAE

Name: Mr. JakchaiThawornwatthanasirikul

Date of Birth: Feb 5, 1989

Nationality: Thai

University Education:

2008–2012 Bachelor Degree of Chemical Engineering (Second Class Honors), Faculty of Engineering, Kasetsart University, Bangkok, Thailand

Work Experience:

2011	Position:	Engineering Internship (2 months)
	Company name:	SCG Cement
		Saraburi, Thailand
2013-2014	Position:	Technical Engineer (1 year 5 months)
	Company name:	Thai Bridgestone Co., Ltd.
		Pathumthani, Thailand

Proceedings:

1. Thawornwatthanasirikul, J., Kitiyanan, B., Rangsunvigit, P., and Kulprathipanja, S. (2017, May 23) Methane adsorption by carbon molecular sieve derived from polycarbonate and polyaniline. Proceedings of the PPC & PETROMAT Symposium 2017, Bangkok, Thailand.